Applied Catalysis B: Environmental 176 (2015): 249 - 265

DOI: http://dx.doi.org/10.1016/j.apcatb.2015.04.003

Preparation of magnetite-based catalysts and their application in heterogeneous Fenton oxidation –A review

Macarena Munoz, Zahara M. de Pedro, Jose A. Casas and Juan J. Rodriguez*

Seccion Departamental Ingenieria Quimica, Universidad Autonoma de Madrid, Ctra. Colmenar km 15, 28049 Madrid, Spain

*Corresponding author phone: +34 91 497 3991; fax: +34 91497 3516; e-mail: macarena.munnoz@uam.es

Keywords: Fenton; CWPO; iron mineral; magnetite; ferromagnetic catalyst; magnetic nanoparticles.

Abstract

This study presents a critical review on the application of magnetite-based catalysts to industrial wastewater decontamination by heterogeneous Fenton oxidation. The use of magnetic materials in this field started only around 2008 and continues growing increasingly year by year. The potential of these materials derives from their higher ability for degradation of recalcitrant pollutants compared to the conventional iron-supported catalysts due to the presence of both Fe(II) and Fe(III) species. In addition, their magnetic properties allow their easy, fast and inexpensive separation from the reaction medium. The magnetic materials applied up to now can be classified in three general groups: magnetic natural minerals, *in-situ*-produced magnetic materials and ferromagnetic nanoparticles. A survey of the catalysts investigated so far is presented paying attention to their nature and competitive features in terms of activity and durability.

Contents

1. Introduction

The treatment of industrial wastewaters is a long-standing problem of environmental relevance. Many industrial activities and most in particular the chemical ones generate wastewaters containing a wide variety of persistent, toxic and non-biodegradable organic pollutants such as phenol, benzene, anilines or chlorophenols, among other. Those streams must be treated as inexpensively as possible in a safe and environmentally friendly manner, preferably by processes that are easy to operate on-site. The ultimate goal of the treatment is that the resulting effluent meets the discharge regulations but looking also for potential recycling and reuse.

Advanced oxidation processes (AOPs) have shown great potential for the treatment of industrial wastewaters [1-7]. These processes operate at near ambient temperature and pressure involving the generation of hydroxyl radicals in sufficient quantity to allow oxidizing the organic pollutants.

The hydroxyl radical constitutes one of the most powerful oxidant (E^0 = 2.73 V), much stronger than other conventional oxidizing species such as hydrogen peroxide (E^0 = 1.31 V) or ozone (E^0 = 1.52 V) [8]. That extraordinarily reactive species attacks non-selectively most of the organic molecules with high rate constants usually in the order of 10^6-10^9 M^{-1} s^{-1} [9]. Due to their high reactivity and low selectivity hydroxyl radicals are quickly consumed and must be continuously generated *in-situ* during the process. Attending to the way of generating hydroxyl radicals the AOPs are usually classified as chemical, electro-chemical, sono-chemical and photochemical processes.

1.1. The Fenton process

The Fenton process is one of the most cost-effective AOP [9-13]. It was discovered more than one hundred years ago by Henry J. Fenton, who reported that H_2O_2 could be activated by iron salts to oxidize tartaric acid [14]. However, this process was not applied for the removal of organic pollutants until the late 1960s [15]. The renewed interest of researchers for this classic reactive system began only

around 1990 [16] and continues nowadays since the number of investigations devoted to its application to wastewater treatment is still rising considerably (Figure 1).

The conventional Fenton process is based on the generation of hydroxyl radicals from the decomposition of hydrogen peroxide in the presence of ferrous iron (Fe^{2+}) at acidic conditions (Eq. (1)) yielding Fe^{3+}. Additionally, these ferric ions react with hydrogen peroxide producing hydroperoxyl radicals and regenerating the catalyst, the ferrous ions (Eq. (2)). If the reaction is initiated by ferric as opposed to ferrous iron the process is commonly referred as "Fenton-like" although it is a cycle and both species are present simultaneously regardless the starting ion. Those are the general reactions commonly used to describe the basic Fenton mechanism. However, the process is much more complex and includes many other reactions [8, 16-18], which could be classified in the three general groups of free-radical processes: initiation, propagation and termination reactions (Table 1). The main goal of the treatment of industrial wastewaters by Fenton oxidation is to achieve the degradation of the organic pollutants taking advantage of the initiation and propagation reactions and trying to avoid the appearance of undesirable termination reactions, where radicals react among them or with iron or hydrogen peroxide instead of oxidizing in depth the organic pollutants.

The oxidation of organic pollutants leads to the formation of intermediate species, which can be further oxidized up to CO_2, H_2O and (if the pollutant contains heteroatoms) inorganic salts. Thus, the overall process can be schematically described by the following paths:

$$Pollutants + H_2O_2 \xrightarrow{Fe^{2+}/Fe^{3+}} intermediates \quad (14)$$

$$intermediates + H_2O_2 \xrightarrow{Fe^{2+}/Fe^{3+}} CO_2 + H_2O + inorganic\ salts \quad (15)$$

The advantages of the Fenton process relative to other oxidation techniques are the simplicity of equipment and the mild operating conditions usually employed. Hydrogen peroxide is safe and easy to

handle, and poses no lasting environmental threat, since it readily decomposes to water and oxygen. Likewise, iron is inexpensive, safe and environmentally friendly.

The Fenton process has been successfully applied to the treatment of highly polluted wastewaters such as cosmetics [4, 19], olive-mill [20, 21], chemicals [4], pulp and paper [11], power plants [5] or sawmills [6], among others [22].

The first step in the Fenton process treatment is the homogenization of the raw wastewater by mechanical agitation and the adjustment of the pH. The resulting effluent is fed to the reactor and once the desired temperature is reached the iron solution and hydrogen peroxide are directly added. The catalyst and hydrogen peroxide doses as well as the temperature and the reaction time must be established upon experimentation whereas the optimum pH is around 3 [23]. Only a small amount of $Fe^{2+/3+}$ is required because it is regenerated during the process (Eq. (1-2)), being commonly used 1 part of iron per 4-25 parts of hydrogen peroxide (w/w) [24], while the optimum dose of oxidant is frequently the stoichiometric amount for complete oxidation, namely mineralization [25, 26]. Although most of the works dealing with Fenton oxidation have been carried out at mild conditions, Zazo et al., (2011)[27] have recently demonstrated that increasing the temperature, up to 120 ºC, clearly improves both the oxidation rate and the degree of mineralization of the pollutants. The Fenton effluent is finally neutralized with NaOH, and thus iron complexes precipitates as $Fe(OH)_3$. A final filtration unit to remove fine aggregates may be necessary to meet discharge or further water reuse requirements. A general flow scheme of the Fenton process is depicted in Figure S1 of the Supplementary Material.

The generation of undesirable iron sludge at the end of the process represents one of the main drawbacks of this process. The costs associated to its treatment and disposal can represent up to 10-50% of the total operating cost of the wastewater treatment [4, 8]. Thus, reducing the amount of sludge is imperative and has stressed the importance of using iron-bearing solid catalysts in the process in order to avoid the continuous loss of catalyst associated to the homogeneous Fenton process.

1.2. Heterogeneous Fenton process

Although the Fenton process has shown to be effective for the treatment of a diversity of industrial wastewaters it suffers some drawbacks that limit a more extended application: sludge generation, the need for pH adjustment before and after reaction and the loss of the catalyst in the effluent. In this context, the use of solid catalysts in the so-called catalytic wet peroxide oxidation (CWPO) or heterogeneous Fenton oxidation is a promising alternative. That is why the interest of the scientific community in this subject has increased greatly in recent years (Figure 2).

The use of supported catalysts allows increasing the surface area of the metal species by providing a matrix that enables their dispersion as very small particles. It diminishes the sintering of the active phase and improves the thermal and chemical stability of the catalyst. As can be seen in Figure 3a, a wide range of materials have been tested as supports or catalysts themselves in CWPO. Pillared clays represent the most frequent, followed by zeolites and silica. However, low attention has been paid so far to the use of iron oxides or natural iron minerals. That metal is by far the most commonly used as active phase in Fenton-type oxidation although many others have been also investigated, as depicted in Figure 3b.

Despite the advantages of CWPO with regard to the conventional Fenton process, its commercial application to wastewater treatment has been restricted so far since unfortunately most of the catalysts studied have shown moderate activity but low stability. The main reasons are related to poisoning, reduction of the catalyst surface and, overall, leaching of iron [28-32]. Thus, the development of more active and stable catalysts represents nowadays one of the most important challenges in CWPO. Promising results have been recently obtained with iron supported on γ-Al_2O_3 catalysts (Fe_xO_y/γ-Al_2O_3), which have proved to be highly active and stable for the treatment of phenolic compounds [33, 34] and real industrial wastewater [2]. Those catalysts showed a remarkable stability in long-term continuous

experiments (100 h) with limited Fe leaching (<3% of the initial loading), the most long standing shortcoming of CWPO so far. In the same line, Taketa et al. (2014)[35] have also reported a high stable process using a mixed material clay/Fe calcined at high temperatures (500-700 ºC). The catalyst showed no loss of activity after five consecutive batch studies.

2. Application of magnetic materials as catalysts in heterogeneous Fenton oxidation

In addition to the stability of the catalyst, its recovery and reusability represent a key issue regarding its potential application. CWPO is usually carried out with the catalyst as suspended powdered particles, then requiring further separation to recover the catalyst from the reaction medium. Therefore, the development of magnetic catalysts provides an interesting solution, allowing easy, fast and inexpensive separation upon the application of a magnetic field (magneto-sedimentation), simplifying its recovery and reusability (see the flow chart of the process Figure S1 of the Supplementary Material).

The magnetic materials tested as catalysts in CWPO can be classified in three general groups: magnetic natural minerals, supported magnetite, and ferromagnetic nanoparticles (MNPs). As can be seen in Figure 4a, the interest of the scientific community on this field started only around 2008 and has been increasingly growing in the last years. Before that, several attempts studying the potential application of magnetite and other natural minerals as catalysts in Fenton oxidation were carried out [36-40]. However, the first work published devoted uniquely to magnetite as CWPO catalyst is that reported by Zhang et al. (2008)[41], who studied the degradation of phenol by Fenton oxidation using ferromagnetic nanoparticles (MNPs). These authors claimed that MNPs represent a promising alternative to the conventional catalysts used in CWPO due to their higher activity as well as their easy recovery and further reusability. As can be seen in Figure 4b, MNPs have received considerably higher attention so far. Figure 5 summarizes the materials and preparation methods used in the investigation of magnetic catalysts for CWPO, which will be described in detail in the subsequent sections.

2.1. Magnetic natural minerals

The application of natural minerals as catalysts in CWPO is attractive due to their wide availability and low cost. However, although their efficiency has been clearly demonstrated [36, 40, 42, 43], the potential of iron-oxide minerals to catalyze the oxidation of organic pollutants has been scarcely studied so far. The most widely studied minerals are goethite [36, 42, 44], hematite [40, 42], ferrihydrite [40, 42], pyrite [40], lepidocrocite [40] and magnetite [40]. Among them, the application of magnetite (Fe_3O_4) as catalyst in heterogeneous Fenton oxidation is nowadays gaining considerable attention due to its relatively high abundance and low cost together with its easy magnetic separation from the reaction medium [45]. Furthermore, magnetite contains both Fe(II) and Fe(III) species, which according to Eq.(1-2) should have a positive effect on the catalytic activity [8].

Kwan and Voelker (2003)[36] studied the rates of generation of hydroxyl radicals by different mineral-catalyzed Fenton systems concluding that Fe(III) oxides are catalytically less active than their Fe(II) counterparts. Matta et al. (2007)[40] showed that Fe(III) oxides (hematite, goethite, lepidocrocite and ferrihydrite) were less effective in the degradation of 2,4,6-trinitrotoluene than those minerals containing both Fe(II) and Fe(III), such as magnetite and pyrite. Likewise, Hanna et al. (2008)[46] also found that magnetite yielded higher methyl orange oxidation rate normalized to surface area than maghemite or goethite.

Accordingly with its outstanding properties, magnetite is by far the natural magnetic mineral most widely used as catalyst in CWPO [47] whereas other magnetic materials such as maghemite (γ-Fe_2O_3) and δ–FeOOH variants have received considerably lower attention [45]. Magnetite is a spinel iron oxide with chemical structure $(Fe(III))_{tet}[Fe(II)Fe(III)]_{oct}O_4$ where Fe(III) ions occupy equally both octahedral and tetrahedral sites and Fe(II) ions are placed only in octahedral sites. Due to its redox properties, magnetite provides high activity in oxidation processes. So far, it has been successfully tested in the oxidation of a wide variety of non-biodegradable organic pollutants such as trinitrophenol [40], pentachlorophenol [48], phenol [49], tetrabromobisphenol-A [50], various dyes [51] and polycyclic

aromatic hydrocarbons [52]. Maghemite presents the same structure as magnetite, it is also spinel ferrite and ferromagnetic. However, due to absence of Fe(II), its catalytic activity is expected to be lower than that of magnetite [45]. δ–FeOOH and its poorly natural counterpart, feroxyhyte (δ'–FeOOH), have structures based on the CdI_2 and disordered CdI_2 models, respectively [45]. They have received also little attention since Fe oxides (magnetite, maghemite and hematite) have shown to be more active than Fe (hydr)oxides in the studies carried out so far [45, 53]. Table 2 summarizes the work done on the application of magnetite-based natural minerals in CWPO up to now.

The efficiency of CWPO with iron minerals has been found to depend greatly on the dissolution of iron from the solid [40, 43, 44, 48, 54]. Therefore, the iron mineral is used as dissolved iron source and the oxidation proceeds mostly via homogeneous Fenton. However, it has to be mentioned that the kinetics is considerably slower than that of conventional Fenton. Xue et al. (2009)[48] investigated the degradation of pentachlorophenol with magnetite under ambient conditions, analyzing the effect of some chelating agents, like ethylenediaminetetraacetic acid (EDTA), carboxy-methyl-cyclodextrin (CMCD) oxalate, tartrate, citrate and succinate. They concluded that those agents favor the dissolution of iron from the solid, thus promoting the occurrence of homogeneous reaction. Almost complete conversion of pentachlorophenol was achieved but after 9 h reaction time and a significant concentration of dissolved iron (14 mg L^{-1}) was measured. Consistent with these results, Matta et al. (2008)[55] showed that the addition of EDTA and CMCD improved remarkably the conversion of 2,4,6-trinitrophenol in the presence of magnetite from 25 to 50 and 62%, respectively.

In this context, searching for more active and stable minerals capable of accomplishing the oxidation with negligible iron leaching and at higher degradation rates is a challenge. So far vanadium-titanium magnetite has shown to be a highly active and stable mineral in the oxidation of Acid Orange II under mild conditions [51]. Complete conversion of that species was achieved in 4 h reaction time, being the process governed by heterogeneous Fenton oxidation. A slight decrease of catalytic activity was observed upon three consecutive runs, which was attributed to small leaching of iron from the solid.

More recently, Zhong et al. (2012)[50] also claimed the high stability and reusability of titanomagnetite, which retained its activity after three cycles in UV/Fenton oxidation of tetrabromobisphenol-A. Although data on their stability are not available, Aravena et al. (2010)[56] showed that oxide-rich sand fractions from magnetic Ultisols (Metrenco: Fe_2O_3 (57%), TiO_2 (3.1%), MnO_2 (1.6%); Collipulli: Fe_2O_3 (57%), TiO_2 (3.1%), MnO_2 (1.6%)), derived from volcanic materials, are also effective catalysts.

Despite the fact that several magnetic minerals have shown to be fairly stable in the process, the degradation rates observed are still far from those of homogeneous Fenton oxidation under similar operating conditions [27]. With the aim of improving the activity of the catalysts and thus, increasing the oxidation rate, the effect of including other metals into the magnetite structure by isomorphic substitution of Fe has been studied by several authors [37-39, 57, 58]). Costa et al. (2006)[37] showed that the presence of Co or Mn produced a substantial increase of the activity of magnetite, whereas Ni inhibited H_2O_2 decomposition in the CWPO of methylene blue. Similarly, Baldrian et al. (2006)[38] found that magnetite doped with Co, Cu or Mn allowed the effective oxidation of various synthetic dyes, maintaining its activity upon successive runs. They concluded that the presence of Mn and Co promotes the decomposition of H_2O_2 into $HO\cdot$ radicals and accelerate electron transfer giving rise to a more efficient regeneration of Fe(II). In the same line, Magalhaes et al. (2007)[39] demonstrated that the presence of small amounts of Cr in the magnetite structure caused a significant increase of activity in the oxidation of azo dyes with complete discoloration and high mineralization. However, the main advantage of natural magnetic minerals in Fenton oxidation derives from their direct application without any modification, thus implying a fairly low cost. In this context, the intensification of the process could represent an interesting way of enhancing the catalytic performance. So far, all the studies carried out have been related to the use of natural minerals at ambient temperature. Nevertheless, recent findings in Fenton oxidation have shown that increasing the temperature leads to a more efficient consumption of H_2O_2 which indicates an enhanced iron-catalyzed H_2O_2 decomposition into radicals, thus clearly improving the oxidation rate and mineralization [4, 27]. For that reason, some commercial applications

of the Fenton process at industrial scale are currently performed at temperatures up to 120 ºC (OHP®, MFC-Foret®). Accordingly, we have recently studied the effect of increasing the temperature (25-90 ºC) in the decomposition of H_2O_2 catalyzed by three natural minerals – hematite, magnetite and ilmenite [59]. Ilmenite is a crystalline iron titanium oxide ($FeTiO_3$) where Fe and Ti occupy alternating layers. It has not been previously used as catalyst in CWPO probably due to the low rate observed for H_2O_2 decomposition [60], and so far has only been successfully tested in the degradation of various organic pollutants by photocatalysis [60, 61]. However, due to its magnetic properties and low cost it could also represent an interesting catalyst for CWPO.

According to our results, increasing the temperature represents an interesting alternative to improve the rate of the process. Whereas at ambient temperature the minerals tested yielded very low rates of H_2O_2 decomposition, almost complete conversion was achieved at 90 ºC. To gain further insight on the catalytic performance of the three aforementioned minerals, they were also tested in the oxidation of phenol at 75 ºC, paying special attention to iron leaching. Complete conversion of phenol was achieved in 2 h reaction time, with fairly high mineralization, above 70%, after 4 h with the three minerals. The concentration of dissolved iron in the liquid phase was 13, 3 and 1 mg L^{-1} for magnetite, hematite and ilmenite, respectively, representing as less as 1.8, 0.5 and 0.3% of the initial load. Although magnetite suffered the highest iron leaching, it was also the mineral showing the best stability upon three sequential runs, maintaining or even slightly increasing the percentage of mineralization. These results were directly related to the amount of iron leached, which decreased upon the three successive runs (13, 6 and 4 mg L^{-1} measured in the liquid phase). Therefore, in the first run, homogeneous Fenton contribution was important due to the concentration of dissolved iron in the reaction medium, giving rise to high rates of hydroxyl radical generation, which affected negatively to the efficiency of the process. In the subsequent runs, where iron leaching was lower, the homogeneous contribution was less and less important, allowing slight improvement of mineralization. Hematite yielded slight decreases of mineralization upon the three sequential runs whereas ilmenite, surprisingly, showed negligible activity

upon the second and third runs due to strong deactivation, which seems to be related to a significant change on the structure of the mineral, as observed by XRD. It has to be highlighted the potential of magnetite as CWPO catalyst under the testing conditions due to its high activity and remarkable stability. Moreover, the mineralization percentage achieved was even higher than the obtained upon homogeneous Fenton oxidation under similar working conditions [27].

2.2. Magnetic catalysts prepared by *in-situ* synthesis of magnetite

The development of magnetic catalysts by *in-situ* synthesis of magnetite has been gaining importance in the last few years. The octahedral structure of magnetite can easily accommodate both Fe(II) and Fe(III), which means that Fe(II) can be reversibly oxidized and reduced back in the same position. Therefore, the magnetite-based catalysts present a higher potential for degradation of recalcitrant pollutants than the conventional iron-supported catalysts where the active phase contains predominantly Fe(III), mostly as hematite (Fe_2O_3) [2, 29-31, 62].

In contrast to the complexity, high cost and difficult scale-up of MNPs synthesis, conventional methods represent a simple and effective way to prepare magnetic catalysts. The main steps commonly followed in the preparation of those magnetic catalysts are shown in Figure S2 of the Supplementary Material. Briefly, an aqueous solution of the iron salt is deposited on the support, which is subsequently subjected to different thermal treatments addressed to allow the formation of magnetite, and thereby, the development of magnetic properties in the solid. So far, activated carbon, alumina and pillared clays have been the main supports used for the preparation of this kind of magnetic catalysts as summarized in Table 3.

Activated carbon has been, by far, the most studied support, probably due to its favorable properties such as high surface area, well developed porous structure, variable surface composition, good chemical resistance and acceptable cost [29, 30]. Nguyen et al. (2011)[63] prepared a magnetic carbon catalyst by

incipient wetness impregnation of activated carbon with an aqueous solution of $Fe(NO_3)_3 \cdot 9H_2O$, followed by drying at room temperature and heat treatment at 600 ºC under N_2 atmosphere for 1 h. The presence of magnetite was confirmed by XRD, showing the magnetic activated carbon a saturation magnetization (M_S) value of 6 emu g^{-1}. Thereby, the catalyst can be manipulated by a device providing a magnetic field. The catalyst (2.5 g L^{-1}) was tested for methyl orange (50 mg L^{-1}) oxidation at 30 ºC and pH 4. Complete conversion of that compound and close to 60% mineralization were achieved after 2 h reaction time. The catalyst was fairly stable upon three sequential runs although a slight loss of activity was observed due to small iron leaching. A similar preparation procedure was followed by Tristao et al. (2014)[64], who synthesized a carbon matrix containing Fe_3O_4 particles and applied it to the oxidation of methylene blue at ambient conditions. The catalyst was prepared by wetness impregnation using aqueous solutions of $Fe(NO_3)_3 \cdot 9H_2O$ with 1, 4, and 8 wt. % Fe at pH 1 (HCl). After evaporation, the solid samples were thermally treated at 400, 600 and 800 ºC in N_2 atmosphere for 1 h. XRD analyses confirmed the presence of Fe_3O_4 with crystallite sizes between 13 and 20 nm in the catalyst treated at 400 ºC, whereas those treated at higher temperatures contained metallic iron and Fe_3C. Under the optimum operating conditions, methylene blue (200 mg L^{-1}) was almost completely removed (95%) after 3 h reaction time using 4.3 g L^{-1} of catalyst (8%Fe-400) at pH 6.

Chun et al. (2012)[65] synthesized magnetite mesocellular carbon foam (MSU-F-C) by wet impregnation using an ethanolic solution of $Fe(NO_3)_3 \cdot 9H_2O$ as iron precursor. In this case, after evaporation of ethanol under stirring, the resulting solid was heated to 400 ºC for 4 h under H_2/Ar atmosphere. The XRD patterns confirmed the presence of magnetite in the catalyst, which showed a high M_S (32 emu g^{-1}). An average particle size of 15 nm for Fe_3O_4 was reported. The activity of the catalyst (0.1 g L^{-1}) was tested in the CWPO of phenol (10 mg L^{-1}) at ambient conditions and pH 3. At the end of the experiments (4 h), almost complete conversion of phenol (95%) was achieved. The homogenous Fenton contribution due to dissolved iron from the catalyst was very low (<0.6 mg L^{-1}) and non-appreciable loss of activity was observed after multiple consecutive runs.

The synthesis of magnetic carbon-based catalysts can be also carried out from Fe-bearing materials as precursors, looking for improved stability. Following this line, Gu et al. (2012)[66] synthesized a magnetic porous carbon containing Fe_3O_4 (FPC) from sewage sludge solids upon carbonization and activation without extra addition of iron, given the already high content of the precursor. Pyrolysis was carried out at different temperatures (600, 800 and 1000 ºC) in N_2 atmosphere for 2 h. The FPC600 was selected as optimum for CWPO due to its well-developed porous structure, with a higher contribution of mesoporosity. Its M_s was 8.7 emu g^{-1} and the XRD pattern revealed the presence of Fe_3O_4, Fe_3C and α-Fe. The dye 1-diazo-2-naphtol-4-sulfonic acid (250 mg L^{-1}) was tested as target pollutant for CWPO experiments, which were performed with 0.5 g L^{-1} catalyst under mild conditions (25 °C) at pH 5. The catalyst showed a high activity, allowing almost complete conversion of the dye (97%) and a high mineralization (87%) after 4 h reaction time. The stability of the catalyst was demonstrated upon three sequential applications although a slight loss of activity was appreciated due to some iron leaching (0.77% of the initial iron content). The same research group compared in a following study the efficiency of the catalyst with that of Fe_3O_4 nanoparticles under the same operating conditions, finding that conversion and mineralization were around two times lower with the nanoparticles [67]. This better performance of the magnetic catalyst was attributed to a higher dispersion of active centers as well as to the adsorption by the carbonaceous support.

In contrast to the conventional methods previously shown, Yang et al. (2014)[68] have recently synthesized a magnetic NdFeB-activated carbon catalyst by vacuum impregnation, obtaining also good results in terms of activity and stability. Briefly, the magnetic NdFeB powder was sprayed onto the wet AC under vacuum leading to the formation of NdFeB magnetic activated carbon with a saturated magnetization of 18.11 emu g^{-1}, which allowed easy separation from the reaction medium. The activity and stability of the catalyst were tested in the degradation of methyl orange. Under the optimum operating conditions (20 mg L^{-1} methyl orange, 10 g L^{-1} catalyst, 20 mg L^{-1} H_2O_2, pH 3 and 20 ºC), 98%

conversion was achieved after 1 h reaction time and the catalyst maintained its activity almost unchanged after 5 cycles with negligible iron leaching.

Pillared clays have become an important class of materials with potential application as catalysts due to their thermal and mechanical stability. Particularly, pillared clays containing mixed aluminum/iron oxide pillars are known as promising heterogeneous Fenton catalysts [31, 69-73].

Tireli et al. (2014)[74] have recently developed a magnetic pillared clay catalyst for its application in methylene blue oxidation. The pillared clay was prepared by inserting Na^+ into montmorillonite clay, and further exchanging by Fe^{3+}. After storage in an acetic acid atmosphere at room temperature for 72 h, it was then heated in air atmosphere up to 500 ºC at a heating rate of 10 ºC/min. The solid remained at 500 ºC for 1 h. The resulting material showed magnetic properties due to the presence of maghemite iron phase, confirmed by XRD and XPS. The catalyst displayed a good adsorption capacity for methylene blue. Upon CWPO only some slight extra decoloration of methylene blue was achieved. Under photo-Fenton conditions, the material showed a better performance, achieving complete decoloration in 90 min. In the same line, Wang et al. (2014a)[75] prepared magnetic bentonite by co-precipitation using iron salt and Al-pillared bentonite. Characterization of the magnetic bentonite by XRD, SEM and BET confirmed the presence of magnetite nanoparticles on the surface and a high surface area (129.4 m^2 g^{-1}). The catalyst was tested in the degradation of Orange II by UV-Fenton. Under the optimum conditions (0.6 g L^{-1} magnetic bentonite, 714 mg L^{-1} H_2O_2, pH 3 and 40 ºC), complete conversion of Orange II (175 mg L^{-1}) was achieved after 3 h reaction time. The catalyst showed an acceptable stability.

Alumina (Al_2O_3) is widely used as catalyst support due to its mechanical, electrical and chemical stability as well as its relatively low cost. In contrast to carbon-based catalysts, alumina-supported ones have shown a considerably higher stability in CWPO [2]. In a recent contribution [34], we prepared a $Fe_3O_4/\gamma\text{-}Al_2O_3$ catalyst adding a reduction stage in H_2 atmosphere (2 h at 350 ºC) to the preparation

procedure previously described by Bautista et al. (2010, 2011)[2, 33] to synthetize a $Fe_2O_3/\gamma\text{-}Al_2O_3$ catalyst. That additional step was addressed to reduce Fe_2O_3 to Fe_3O_4 and thus develop magnetic properties in the catalyst. The activity and stability of this new magnetic catalyst were compared with those of the conventional $Fe_2O_3/\gamma\text{-}Al_2O_3$ one. The presence of hematite (Fe_2O_3) and magnetite (Fe_3O_4) in the conventional and new catalysts, respectively, was confirmed by XRD, XPS and Mössbauer spectroscopy. The iron nanoparticles presented a wide range of sizes within 5-45 nm, showing a mean diameter of 25 and 33 nm for $Fe_2O_3/\gamma\text{-}Al_2O_3$ and $Fe_3O_4/\gamma\text{-}Al_2O_3$, respectively. The magnetic catalyst presented a M_S value of 2.24 emu g^{-1}, which allowed easy separation from the reaction medium by a magnet. The activity and stability of both catalysts (1 g L^{-1}) were tested in CWPO of 4-chlorophenol, 2,4-dichlorophenol and 2,4,6-trichlorophenol (100 mg L^{-1}) at 50 ºC and pH 3. Complete dechlorination of all the chlorophenols tested was achieved with mineralization above 70% after 4 h reaction time. The residual by-products were short-chain organic acids without significance in terms of ecotoxicity. The magnetic catalyst decomposed H_2O_2 about three times faster than the conventional one (7.3×10^{-3} and $2.4 \times 10^{-3} min^{-1}$, respectively). Thus, the degradation rate of the target pollutants was also faster. Both catalysts showed a high stability upon long-term continuous experiments (100 h), being the loss of iron below 5%. The BET surface area remained unchanged and only small amounts of residual carbon-containing species (≈1.2 wt.-%) were detected on the catalyst surface.

The magnetite-based catalysts developed so far have shown to be fairly active and stable in CWPO of different organic compounds, being the degradation rates considerably higher than those previously reported with the hematite counterparts. However, the oxidation rates are still far below those obtained by conventional homogeneous Fenton oxidation under similar operating conditions. For the sake of improving the rate of the process, we have recently explored the effect of temperature within 50 to 90 °C [76]. The magnetic catalyst (1 g L^{-1}) allowed complete degradation of chlorophenol (100 mg L^{-1}) and 90% TOC reduction after 1 h reaction time at pH 3 and 90 ºC temperature. That degree of mineralization was considerably higher than the obtained upon Fenton oxidation (60%) under the same

operating conditions. Iron leaching from the catalyst was even lower than the observed at 50 ºC (2.5 and 0.5 mg L^{-1} Fe^{3+} at 50 and 90 ºC, respectively) because the concentration of oxalic acid was significantly reduced. This acid has proved to provoke a negative effect on the stability of supported Fe catalysts due to metal leaching [29]. Besides, the catalyst showed a remarkable stability upon three sequential runs without significant loss of activity and was easily separated from the reaction medium because of its magnetic properties. Thus, the use of the magnetic $Fe_3O_4/\gamma\text{-}Al_2O_3$ catalyst at high temperature (90 ºC) clearly represents an interesting alternative to homogeneous Fenton oxidation and opens the door for a more efficient application of magnetite-based catalysts.

2.3. Ferromagnetic nanoparticles

The use of MNPs in heterogeneous catalysis has gained considerable attention in the last few years. MNPs have been reported as catalysts in many reactions such as Fischer-Tropsch or Haber-Bosch as well as in environmental catalysis and peroxidase-like activities [77]. Particularly, MNPs, mainly zero-valent iron (nZVI), magnetite (Fe_3O_4) and maghemite ($\gamma\text{-}Fe_2O_3$), have received much interest for the treatment of polluted water or subsurface environments during the last decade [78-82]. Since 2008, MNPs are being also applied in Fenton-like oxidation and represent nowadays a new generation of catalysts for that technology. As observed in Figure 4b, most of the works published dealing with the application of magnetic catalysts in Fenton oxidation are focused on the use of MNPs. Their importance is associated to their inherent properties, which can differ from those of the macroscopic or bulk forms of the same material [83]. Furthermore, their activity and selectivity are strongly dependent on their size, shape and surface structure, as well as on their bulk composition, which can be appropriately tuned during their synthesis.

The synthesis of MNPs can be carried out by different methods such as co-precipitation [41, 84], microemulsion [85], hydrothermal [86, 87] or sonochemical synthesis [88], among other [83].

Co-precipitation is, by far, the most commonly applied method [83, 89]. It is based on mixing ferric and ferrous ions, commonly in a 1:2 molar ratio, in highly basic solutions at room or higher temperature. The size and shape of MNPs can be modified by selecting the type of salt, the ferric to ferrous ions ratio, the temperature, pH and the ionic strength of the medium [89]. The main drawback of this method is the wide particle size distribution achieved, which usually requires secondary size selection. A microemulsion is a thermodynamically stable isotropic dispersion of two immiscible phases, frequently water and oil, in the presence of a surfactant. Shape- and size- controlled MNPs can be synthesized by this method due to the formation of self-assembled structures such as spherical micelles or lamellar phases [89]. However, several washing steps and further stabilization treatments are required to avoid the aggregation of the MNPs. Hydrothermal synthesis includes various wet chemical technologies of crystallizing the substance at high temperature (130 to 250 ºC) and pressure (0.3 to 4 MPa). In sonochemical synthesis, MNPs are formed by the implosive collapse of bubbles through acoustic cavitation. The extreme conditions achieved in these hotspots are beneficial for the formation of MNPs and have a shear effect for agglomeration [89]. Thermal decomposition is based on the decomposition of an organic solution phase ($Fe(cup)_3$ (cup = N-nitrosophenylhydroxylamine), $Fe(acac)_3$ (acac = acetylacetonate) or $Fe(CO)_5$) followed by oxidation leading to high-quality monodispersed MNPs. Nevertheless, it requires relatively high temperatures and a complex operation.

Table 4 summarizes the literature works dealing with the application of MNPs in CWPO. They have proved to be highly active catalysts in the oxidation of different organic pollutants such as phenol [41], chlorophenol [90], aniline [91], dyes [88] or emerging pollutants [92-94].

Zhang et al. (2008)[41] applied MNPs as catalyst in CWPO of phenol. The nanoparticles were prepared by co-precipitation and appeared approximately spherical with an average diameter of 13 nm. They showed a M_S value of 65 emu g^{-1}, which is indicative of their strong magnetic character. The CWPO tests were performed at 16 ºC and pH 3, using an initial concentration of phenol of 280 mg L^{-1}, 100 mg L^{-1} MNPs and 2 g L^{-1} H_2O_2. After 3h, a high conversion of phenol (85%) was achieved whereas

mineralization did not exceed 30%. The reusability of MNPs was evaluated upon subsequent use in 5 consecutive cycles including simple regeneration steps which involved sonication and washing with deionized water. After those 5 cycles, the catalytic activity of MNPs remained almost invariable. Similar results were obtained by Wang et al. (2010)[88] in CWPO of Rhodamine B (10 mg L^{-1}) with MNPs (600 mg L^{-1}) at 40 ºC and pH 5. Around 90% conversion was achieved in 1 h, where limited iron leaching occurred. More recently, Sun et al. (2013)[93] studied the degradation of two emerging pollutants, carbamazepine (CBZ) and ibuprofen (IBP), by heterogeneous Fenton-like oxidation with nano-magnetite. Experimental design and response surface methodology were applied to evaluate the effects of pH, H_2O_2 and catalyst doses. The results showed that hydroxyl radical formation by the heterogeneous decomposition of H_2O_2 on the Fe_3O_4 nanoparticle surface plays the dominant role in CBZ and IBP degradation at neutral pH. Under the optimum operating conditions (1.84 g L^{-1} Fe_3O_4, 20.4 g L^{-1} H_2O_2 and pH 7), conversion of CBZ and IBP reached 86 and 83%, respectively.

Although MNPs have shown to be fairly active in CWPO, their stability is still an important challenge since, though there are controversial results, it is generally far from that showed by the catalysts prepared by conventional procedures when the degrees of mineralization achieved are significant (≥40%). The leaching of iron seems to be the most important reason for the stability decay although other issues such as the agglomeration of the nanoparticles as well as their lost during supernatants discharge have to be also considered. Xu and Wang (2012a)[90] used MNPs prepared by co-precipitation, in CWPO of 2,4-dichlorophenol at ambient conditions (30 ºC, pH 3, 100 mg L^{-1} 2,4-dichlorophenol, 1 g L^{-1} MNPs, 0.4 g L^{-1} H_2O_2). The MNPs yielded good results in terms of activity, achieving the complete conversion of the pollutant and TOC reduction above 50% after 3 h reaction time. However, their stability was not satisfactory since the pollutant conversion decreased from 95% to 40% after 5 successive runs. This loss of activity was mainly related to iron leaching (≈10%), but other factors such as reduction of the catalyst surface area, poisoning of the active catalytic sites by adsorbed organic species and aggregation of MNPs were also pointed out. Similarly, Zhang et al. (2009)[91]

studied the oxidation of phenolic and aniline compounds using MNPs prepared by co-precipitation. The oxidation runs were carried out at 35 ºC at neutral pH using 5 g L^{-1} MNPs, 40 g L^{-1} H_2O_2 and 94 mg L^{-1} pollutant concentration. Complete conversion of phenol and aniline were achieved with TOC reduction around 40% after 6 h of reaction. After 8 sequential uses of MNPs, conversion of phenol and TOC were reduced by 20 and 30%, respectively. The main causes of that loss of activity were the agglomeration of MNPs and the fact that MNPs might be lost during the discharge of supernatants. This lack of stability has also been claimed by other authors. Huang et al. (2012)[92] found a decrease of 30% on Bisphenol A conversion after 5 CWPO successive runs. In the same line, Rusevova et al. (2012)[95] observed a 50% reduction on the catalytic activity of MNPs upon 3 sequential uses in CWPO of phenol. In this case, the authors associated the loss of activity to the complexation of iron by organic acids, which blocks active centers or causes a destruction of the active surface structure. Likewise, Ferroudj et al. (2013)[96] attributed the loss of activity upon sequential applications of magnetic maghemite nanoparticles to iron leaching (7.3 mg L^{-1}).

Apart from the stability concerns, the efficiency of the process should be also considered. Most of the works carried out so far using MNPs as catalysts have been characterized by the use of large amounts of H_2O_2, far above the theoretical stoichiometric for complete mineralization of the organic pollutant [88, 91-93, 95, 96]. However, it is well-known that the consumption of this reagent is a critical issue for the economy of the process [4, 27, 97]. Zazo et al. (2011)[27] defined the efficiency on the use of H_2O_2 in Fenton oxidation as the amount of TOC converted per unit of H_2O_2 decomposed and fed (w/w). The last one is more representative since residual H_2O_2 cannot be recovered and, moreover, needs to be removed before discharge due to its toxicity. A representative example of the efficiency achieved with MNPs is the study reported by Zhang et al. (2009)[91] who carried out the oxidation of phenol (72 mg L^{-1} TOC) with 40.1 g L^{-1} H_2O_2, achieving a TOC reduction of 43%. The efficiency in this case is as low as 0.77 mg TOC/g H_2O_2 fed whereas that obtained upon homogeneous Fenton oxidation of the same organic pollutant under similar operating conditions is around 43 mg TOC/g H_2O_2 fed [27].

So far, all the works devoted to the application of MNPs in CWPO have been carried out at near ambient temperatures, which can explain the low efficiencies obtained on the use of H_2O_2. However, as aforementioned, the operation at higher temperatures can significantly enhance the activity and stability of the catalysts in CWPO. Recently, Velichkova et al. (2013)[94] evaluated the activity of nano- and submicro-structure magnetite and nanostructured maghemite (6 g L^{-1}) in heterogenenous Fenton oxidation of paracetamol (100 mg L^{-1}) using 0.95 g L^{-1} H_2O_2 at acidic pH (2.6). The influence of reaction conditions such as temperature, iron and hydrogen peroxide amounts was investigated. They highlighted that increasing temperature from 30 to 60 ºC showed a beneficial effect, concluding that paracetamol mineralization was improved by high temperature and low oxidant dose due to radical scavenging effects. The efficiency of H_2O_2 consumption increased from 13 up to 32 mg TOC/g H_2O_2 fed. Under the optimum conditions, paracetamol was fully converted after 5 h reaction time, with 50% mineralization using nanostructured magnetite as catalyst. All iron oxides exhibited low iron leaching (<1%) and no apparent loss of activity in two successive runs.

2.3.1. Supported ferromagnetic nanoparticles and magnetic composites

Separation of MNPs from solution by magnets has been frequently reported. However, although graphical evidences have shown the feasibility of separation and recovery of MNPs from water [90, 91], no successful real applications have yet been reported [82]. In fact, it has been claimed that the magnetism of MNPs favors their aggregation, thus reducing their dispersibility and activity [77]. Furthermore, nanoparticles can be entrained upon supernatants discharge [91]. Apart from these concerns, the environmental impacts of the application of MNPs in wastewater treatment require special attention associated to the risk of entering the soil and aquatic systems. Thus, some technical advantages of MNPs, like their small size and high reactivity, represent also potential negative factors by inducing adverse cellular toxic and harmful effects, unusual in micron-sized counterparts [82]. According to several studies [82, 98-100], nanoparticles can enter living organisms by ingestion and inhalation and

cause toxic effects in organs and tissues. Moreover, the nanoparticles can interact with pollutants in environmental applications and act as carriers of them into aquatic ecosystems [82, 101-103]. In this context, the immobilization of MNPs onto high-surface-area supports represents an environmentally-friendly solution which would preserve their unique properties, avoiding their potential negative effects.

The application of supported MNPs as well as magnetic composites in CWPO has been widely studied in the last five years and it is still increasingly growing. In particular, they have been gaining importance with respect to unsupported MNPs in the last years. A summary of the works reported so far is collected in Table 5. Two general trends can be distinguished: the synthesis of composites where iron is part of the structure and the impregnation of MNPs onto porous supports. Both methods have shown to be effective for the preparation of active catalysts although differences in stability have been observed.

Costa et al. (2008)[104] investigated the application of Fe^0/Fe_3O_4 composites in heterogeneous Fenton oxidation of methylene blue. The magnetic nanoparticles were synthesized by co-precipitation of the precursor ferric hydroxyacetate followed by thermal treatment at 430 ºC under N_2 atmosphere and reduced at 300, 400 and 500 ºC under H_2 flow (30 mL min^{-1}) for different times (1 min to 4 h). The resulting composites showed a high activity in CWPO of methylene blue. The one reduced at 400 ºC for 2 h allowed 75% mineralization after 2 h reaction time (100 mg L^{-1} methylene blue, 3 g L^{-1} catalyst, 10 g L^{-1} H_2O_2, 25 ºC and pH 6). The composite showed an improved activity of Fe^0 by an efficient electron transfer process which should also have important implications regarding environmental applications of iron. The authors claimed that those results open new perspectives for the development of active heterogeneous Fenton systems by a simple reduction of different iron precursors, e.g. low cost materials such as iron minerals and hazardous wastes like red muds. In the same way, Wang et al. (2014b)[105] used a magnetic ordered mesoporous copper ferrite (Meso-$CuFe_2O_4$) as catalyst for CWPO of imidacloprid. The catalyst presented a good activity, allowing almost complete conversion of imidacloprid (10 mg L^{-1}) and around 30% mineralization after 5 h working at 0.3 g L^{-1} catalyst, 1.36 g

L^{-1} H_2O_2, 30 ºC and pH 3. The activity of the catalyst was associated with the high surface area and large pore size of the composite as well as the redox cycles of Fe(II)/Fe(III) and Cu(I)/Cu(II). That composite showed also a remarkable stability with low iron leaching (<1 mg L^{-1}), maintaining its activity in terms of imdacloprid conversion almost unchanged after 5 consecutive runs. More recently, Lv et al. (2014)[106] established the high stability of magnetic core-shell structured γ-Fe_2O_3@Ti-tmSiO_2 in methylene blue oxidation in 6 successive runs showing negligible iron leaching.

Another interesting work related to the use of composites in CWPO is that reported by Zubir et al. (2014)[77], who investigated the application of graphene oxide-Fe_3O_4 nanocomposites. The magnetic nanocomposites were synthesized by co-precipitating iron salts onto graphene oxide sheets in basic solution. A magnetite load up to 10 wt.-% was beneficial for dispersion of the nanoparticles whereas higher percentages led to their aggregation and the stacking of graphene oxide sheets. The activity of the nanocomposites was evaluated in the degradation of Acid Orange 7. It was demonstrated that the occurrence of strong interfacial interactions (Fe-O-C bonds) between both components gave rise to 20% more conversion of that compound than with unsupported Fe_3O_4 nanoparticles under the same operating conditions (35 mg L^{-1} Acid Orange 7, 200 mg L^{-1} catalyst, 750 mg L^{-1} H_2O_2, 25 ºC and pH 3). This behavior was associated with synergistic structural and functional effects of the combined graphene oxide and Fe_3O_4 nanoparticles. Firstly, the high surface area of exfoliated graphene oxide allows a good dispersion of the magnetic nanoparticles, favoring the mass transfer of reactants towards the active sites. Secondly, graphene oxide favors adsorption due to its similar aromatic ring structure. Thirdly, there are strong interactions between Fe_3O_4 nanoparticles and the graphene oxide via Fe-O-C bonds which enhances electron transfer between the nanoparticles and the semiconductor graphene oxide sheets. Finally, partial reduction on graphene oxide allows the regeneration of Fe(II).

Although composites have shown to be highly active in heterogeneous Fenton oxidation, their stability still represents a challenge in this field. Xia et al. (2011)[107] applied a magnetically separable mesoporous silica nanocomposite as catalyst in the CWPO of phenol. The solid presented highly

dispersed iron species, thus providing enough active sites for CWPO with a remarkable catalytic performance. Oxidation runs were performed with 5 g L^{-1} catalyst and 1.7 g L^{-1} H_2O_2 at 40 ºC and pH 4. Although the catalyst showed a good activity, allowing around 80% phenol conversion after 2 h reaction time, its stability was less acceptable since phenol conversion decreased up to 65% after three sequential uses. That was mainly attributed to iron leaching (≈1 mg L^{-1}). Xu and Wang (2012b)[108] also found a loss of activity upon 6 runs (from 100% to 40% conversion for 1st to 6th runs, respectively) in 4-chlorophenol CWPO with a Fe_3O_4/CeO_2 composite. In this case, iron leaching reached around 12 mg L^{-1}, equivalent to about 1.9% of the initial iron in the catalyst. Likewise, Hou et al. (2014)[87] evidenced a loss of activity (≈10% upon 3 succesive runs) of shape-controlled nanostructures of magnetite-type materials in phenol CWPO at ambient temperature. They attributed the decrease on catalytic activity to partial oxidation of Fe(II) to Fe(III) (the Fe(II)/Fe(III) ratio decreased to 41% from the 53% of the fresh material). Ling et al. (2014)[109] also observed a low stability of magnetic core-shell structural γ-Fe_2O_3@Cu/Al-MCM-41 nanocomposite upon successive application to CWPO of phenol.

In contrast to the relatively low stability of some nanocomposites, Niu et al. (2011)[110] demonstrated that humic acid-coated MNPs present a remarkable stability in CWPO of sulfathiazole, maintaining complete conversion upon 3 successive runs. However, these authors did not provide information about TOC reduction upon sequential cycles. In the same way, Nogueira et al. (2014)[111] investigated the heterogeneous Fenton oxidation of methylene blue with a magnetite/MCM-41 catalyst. Magnetite was prepared by the co-precipitation method and was further incorporated onto the MCM-composite at 5wt.-%. The resulting solid was finally calcined at 600 ºC for 4 h under nitrogen flow. The composite was active in CWPO of methylene blue, allowing 50% conversion of the dye with 43% mineralization. The catalyst was stable upon four consecutive oxidation runs, although no data on iron leaching were reported. Similarly, Cleveland et al. (2014)[112] investigated the heterogeneous Fenton oxidation of Bisphenol A (BPA) using Fe_3O_4 amended onto multi-walled carbon nanotubes

(Fe_3O_4/MWCNT). The catalyst was synthesized by the *in-situ* chemical oxidation and co-precipitation method. Fe_3O_4 exhibited an octahedron crystal structure (100-150 nm) which was well-dispersed onto the MWCNT. The catalyst displayed a remarkable activity for BPA (70 mg L^{-1}) oxidation. Under the optimum operating conditions (0.5 g L^{-1} catalyst, 40 mg L^{-1} H_2O_2, 50 ºC, pH 3) 97% conversion was achieved after 6 h reaction time. These authors also claimed the importance of increasing the operating temperature, enhancing the oxidation rate by a factor of 3.5 by increasing the temperature from 20 to 50 ºC, which allowed using low doses of H_2O_2. After five cycles of Fenton oxidation with the same catalyst, BPA conversion remained unchanged at around 90%, although COD reduction decreased from 35 to 25%, which was attributed to the accumulation of by-products onto the catalyst surface.

3. Advanced applications of magnetite-based catalysts

Challenges in the Fenton-based technologies are addressed to improve the efficiency on the use of H_2O_2 allowing higher percentages of mineralization. As has been discussed, increasing the reaction temperature has demonstrated to be an efficient approach for the intensification of the process. In heterogeneous Fenton the stability of the catalyst in long-term operation is a main issue. In this section, we discuss some advanced strategies to improve the performance of the system when using magnetic catalysts.

3.1. Nano/microreactor systems with confined magnetite

As previously stated, the use of MNPs in bulk solution usually suffers aggregation and vulnerability, which notably lower the catalytic efficiency, thus inhibiting their practical application. On the other hand, although MNPs can be supported onto high-surface-area powdered supports, the catalysts can still be unstable and the catalytic sites can be poisoned readily when directly exposed to the bulk reaction medium. Using a micro- or nanoreactor systems represents an interesting solution to overcome those shortcomings.

Confined micro- and nanoreactors are of growing interest, not only for Fenton technologies, but for many other chemical reaction systems because it is expected to improve conversion rates due to the high local concentrations of reactants. According to several studies [113-116], the catalysts confined in the inner space of nanoreactors or microreactors display enhanced catalytic performance due to the protection of the active sites, which improves the catalytic efficiency. However, only a few works have been published on this topic, overall for the application in Fenton-type oxidation. Cui et al. (2013)[117] synthesized a yolk-shell structured Fe_2O_3@mesoporous-SiO_2 nanoreactor through a simple polymeric carbon-assisted method, which allows tuning the void space size. First, the authors studied the oxidation of methylene blue using the bare Fe_2O_3, which showed relatively low activity, achieving only 20% discoloration after 7h. The mesoporous shell itself led to 30% methylene blue removal during the first hour due to adsorption but not further removal was observed beyond that time. In contrast, the yolk-shell structured Fe_2O_3@mesoporous-SiO_2 nanoreactor was quite active in Fenton oxidation of methylene blue (0.5 g L^{-1} Fe_2O_3, 50 mg L^{-1} methylene blue, 18 g L^{-1} H_2O_2, 25 ºC and pH 5.7). The activity was related to the size of the void space, increasing from 70 to 90% as the void space was increased from 16 to 40 nm. With the latter, complete conversion was achieved although high reaction times were required (10 h). More recently, Zeng et al. (2014)[118] have developed a yolk-shell nanoreactor with a Fe_3O_4 core and Fe_3O_4/C shell, improving previous results due to the presence of magnetite, which is positive for both the activity and recovery of the catalyst. The performance of this nanoreactor exceeded significantly that of the new MNPs under the same operating conditions (0.5 g L^{-1} catalyst, 200 mg L^{-1} 4-chlorophenol, 0.68 g L^{-1} H_2O_2, 25 ºC and pH 4). In this sense, while complete conversion of 4-chlorophenol was achieved in 1 hour, only 28% was reached using bare MNPs. The authors showed that due to the outermost carbon layer and high-magnetization properties, the nanoreactor can be re-used several times with limited iron leaching, thus maintaining its activity almost unchanged.

Research on this field is still incipient but the promising results obtained so far opens the door for further investigations, not only with yolk-shell structures but also through the development of nano/micro-reactors based on the use of crystal fibers decorated with well-dispersed MNPs as has been already done using other metals in similar environmental applications [119].

3.2. *In-situ* production of H_2O_2 and oxidation using magnetic catalysts

H_2O_2 consumption represents, by far, the main operating cost in Fenton-based processes [4, 27, 97] and thus, any reduction is beneficial for the economy of the system. In this context, *in-situ* production of H_2O_2 in the reaction medium with subsequent oxidation of the organic pollutants is of great interest. This approach has been studied so far in a limited extension although several works in the literature have demonstrated its potential [120-122]. In general, H_2O_2 is *in-situ* generated from H_2 and O_2 [123-125], although H_2 can also be replaced by hydrazine, hydroxylamine or formic acid in order to overcome the inherent risk of explosion of that mixture [120, 121]. Yalfani et al. (2011)[121] demonstrated the application of *in-situ* H_2O_2 generated from formic acid and oxygen for different chlorophenols degradation using a bimetallic Pd-Fe/Al_2O_3 catalyst. This solid is able to decompose formic acid at the Pd sites, yielding H_2 and CO_2, and additionally H_2O_2 in the presence of O_2. At the same time, due to existence of iron sites on the catalyst, the H_2O_2 formed can accomplish Fenton oxidation of the organic pollutants. The process was effective since complete converion of chlorophenols (50 mg L^{-1}) with around 70% mineralization were achieved in 6 h reaction time under near ambient temperature (25 ºC) at 1 g L^{-1} catalyst and pH 3, without the addition of external H_2O_2. Moreover, the catalyst showed a promising stability upon 3 sequential applications with negligible Pd or Fe leaching. More recently, Munoz et al. (2013comb.)[126] have developed a magnetic Pd-Fe/γ-Al_2O_3 catalyst which has shown to be highly active and stable in CWPO of chlorophenols and represents also a promising candidate for *in-situ* generation of H_2O_2.

Another well-known approach for *in-situ* generation of H_2O_2 is the application of electro-Fenton. This advanced oxidation process has attracted great attention [127-131] because H_2O_2 can be continuously produced *in-situ* from the reduction of O_2 on the cathode under acidic conditions. H_2O_2 is further decomposed, by the addition of Fe^{2+}, to hydroxyl radicals, which oxidize the organic pollutants. A Pd-based electro-Fenton system allows producing H_2O_2 from the combination of electro-generated H_2 and O_2 on the catalyst surface. The shortcomings of this process are related to the difficult recycle of the expensive Pd catalysts as well as the addition of iron salts, which complicate the implementation of the process and increase the cost. To overcome these limitations, Luo et al. (2014)[131] have recently developed a novel electro-Fenton process based on Pd-catalyzed production of H_2O_2 from H_2 and O_2 by using an integrated catalyst which contains Pd onto magnetic Fe_3O_4 nanoparticles (Pd/MNPs). Previously addition of Fe(II) was commonly used, which complicates the operation and the Pd catalyst was difficult to recover after the treatment. In the new eletrolytic system, H_2O_2 and Fe^{2+} can be produced simultaneously. The system was tested in the degradation of phenol (20 mg L^{-1}), achieving 98% conversion within 60 min under conditions of 50 mA, 1 g L^{-1} Pd/MNPs (5 wt.-% Pd) and pH 3. It was demonstrated that variations of main crystal structure and the magnetic properties of catalysts were minimal after the treatment, but some small amounts of Pd were leached.

4. Prospects and concluding remarks

As has been stated in this review, the application of magnetite-based catalysts represents a promising alternative to homogeneous Fenton oxidation as well as to the use of conventional catalysts in CWPO. The high availability and low cost of magnetic natural minerals make them attractive for that purpose. However, they suffer from high iron leaching which limits their reusability and generates undesired iron sludge after the treatment. In contrast, the *in-situ* formation of magnetite in Fe-supported catalysts by simple treatments represents a more realistic approach due to the high activity and stability of these catalysts. Particularly promising are the most recent results reported with the $Fe_3O_4/\gamma\text{-}Al_2O_3$

catalyst, which allows achieving the high rates of the homogeneous Fenton process but with considerably higher mineralization when the process is operated at high temperature (90 ºC). Under these conditions, the catalyst has shown to be stable, with limited iron leaching and maintaining its magnetic properties after the treatment.

MNPs appear as powerful catalysts and represent so far the main field of study on the application of magnetite-based catalysts in CWPO. The size, shape and surface structure, as well as the bulk composition, can be adequately tuned during the synthesis of MNPs, showing a key role on their subsequent activity and selectivity in CWPO. Nevertheless, their potential application is still limited by a number of shortcomings such as aggregation, with consequent loss of dipersibility, and iron leaching. Moreover, they can be entrained during supernatants discharge. Their immobilization onto a support could be a potential solution; however, the attempts reported so far showed that iron leaching cannot be completely avoided. Therefore, there is room for considerable improvements in this field. The most important challenges point to the use of increasingly smaller sizes of nanoparticles in order to improve the activity and stability of the particles as well as to prevent aggregation.

The results obtained so far with MNPs as CWPO catalyst did not considerably improve those obtained with natural magnetic minerals or catalysts prepared by *in-situ* synthesis of magnetite. Actually, the studies dealing with nanoparticles reported so far have been characterized by the use of fairly high doses of catalyst and H_2O_2, this last well below the stoichiometric amounts. Furthermore, although cost-effective manufacture is clearly stated in the cases of magnetic natural minerals and conventional catalysts with *in-situ* synthesis of magnetite, it must be still demonstrated for the MNPs to allow their widespread application in CWPO.

The use of magnetite-based catalysts in CWPO is still incipient but deactivation due to iron leaching has been identified as one important limitation. On the other hand, the rate of the process should be improved trying to approach to that of homogeneous Fenton oxidation in order to be competitive. This affects mainly to magnetic natural minerals and MNPs since their efficiency has not been demonstrated

yet. This scenario opens the door to the intensification of the process by increasing the temperature, alternative which has been scarcely explored in the literature so far but has shown promising results. The activity but also the stability of the catalysts as well as the achievable mineralization can be considerably improved upon intensification of the process by increasing the reaction temperature. Other advanced strategies such as the use of nano/microreactor systems with confined magnetite as well as the *in-situ* production of H_2O_2 and oxidation using magnetic catalysts have emerged in the last few years allowing enhancing significantly the efficiency in CWPO.

Acknowledgments

This research has been supported by the Spanish MICINN through the project CTQ2013-4196-R and by the CM through the project S2013/MAE-2716.

Figure Captions

Figure 1. Evolution of the number of scientific papers devoted to the application of Fenton oxidation to wastewater treatment. Source: *Scopus (December 2014)*.

Figure 2. Evolution of the number of scientific papers devoted to the application of CWPO to wastewater treatment. Source: *Scopus (December 2014)*.

Figure 3. Literature generated in the field of CWPO by sort of catalytic supports (a) and metal active phase (b) studied. Source: *Scopus (December 2014)*.

Figure 4. Evolution of the number of publications dealing with the application of magnetic materials as catalysts in Fenton oxidation (a) and their distribution according to the kind of magnetic material used (b). Source: *Scopus (December 2014)*.

Figure 5. Trends distinguished in the investigation of magnetic catalysts for CWPO, including the materials and preparation methods involved.

Tables

Table 1. Main reactions involved in Fenton chemistry.

Table 2. Overview of the application of magnetic iron minerals in CWPO for the removal of non-biodegradable organic pollutants.

Table 3. Summary of the works reported in the literature relative to the synthesis of magnetic catalysts by *in-situ* growth of magnetite and their application in CWPO.

Table 4. Summary of the studies devoted to the application of unsupported MNPs in CWPO.

Table 5. Summary of the application of supported MNPs and magnetic composites in Fenton oxidation.

References

[1] F. Germirli Babuna, S. Camur, I.A. Alaton, O. Okay, G. Iskender, Desalination 249 (2009) 682-686.

[2] P. Bautista, A.F. Mohedano, N. Menéndez, J.A. Casas, J.J. Rodriguez, Catalysis Today 151 (2010) 148-152.

[3] X. Zhao, J. Qu, H. Liu, C. Wang, S. Xiao, R. Liu, P. Liu, H. Lan, C. Hu, Bioresource Technology 101 (2010) 865-869.

[4] G. Pliego, J.A. Zazo, S. Blasco, J.A. Casas, J.J. Rodriguez, Industrial & Engineering Chemistry Research 51 (2012) 2888-2896.

[5] G. Pliego, J.A. Zazo, J.A. Casas, J.J. Rodriguez, Journal of Hazardous Materials 252-253 (2013) 180-185.

[6] M. Munoz, G. Pliego, Z.M. de Pedro, J.A. Casas, J.J. Rodriguez, Chemosphere 109 (2014) 34-41.

[7] H. Zangeneh, A.A.L. Zinatizadeh, M. Feizy, Journal of Industrial and Engineering Chemistry 20 (2014) 1453-1461.

[8] E. Neyens, J. Baeyens, Journal of Hazardous Materials B98 (2003) 33-50.

[9] R. Andreozzi, V. Caprio, A. Insola, R. Marotta, Catalysis Today 53 (1999) 51-59.

[10] S. Esplugas, J. Giménez, S. Contreras, E. Pascual, M. Rodríguez, Water Research 36 (2002) 1034-1042.

[11] M. Perez, F. Torrades, X. Domenech, J. Peral, Journal of Chemical Technology and Biotechnology 77 (2002) 525-532.

[12] N. Azbar, T. Yonar, K. Kestioglu, Chemosphere 55 (2004) 35-43.

[13] P. Cañizares, R. Paz, C. Sáez, M.A. Rodrigo, Journal of Environmental Management 90 (2009) 410-420.

[14] H.J.H. Fenton, Journal of the Chemical Society 65 (1894) 899-910.

[15] H.R. Eisenhauer, Journal Water Pollution Control Federation 36 (1964) 1116-1128.

[16] J.J. Pignatello, E. Oliveros, A. MacKay, Critical Reviews in Environmental Science and Technology 36 (2006) 1-84.

[17] R. Chen, J. Pignatello, Environmental Science & Technology 31 (1997) 2399-2406.

[18] C.K. Duesterberg, W.J. Cooper, T.D. Waite, Environmental Science & Technology 39 (2005) 5052-5058.

[19] P. Bautista, A.F. Mohedano, M.A. Gilarranz, J.A. Casas, J.J. Rodriguez, Journal of Hazardous Materials 143 (2007) 128-134.

[20] F. J. Rivas, F. J. Beltran, O. Gimeno, J. Frades, Journal of Agricultural and Food Chemistry 49 (2001) 1873-1880.

[21] M.S. Lucas, J.A. Peres, Journal of Hazardous Materials 168 (2009) 1253-1259.

[22] P. Bautista, A.F. Mohedano, J.A. Casas, J.A. Zazo, J.J. Rodriguez, Journal of Chemical Technology and Biotechnology 83 (2008) 1323-1338.

[23] B.G. Kwon, D.S. Lee, N. Kang, J. Yoon, Water Research 33 (1999) 2110-2118.

[24] M. Pera-Titus, V. García-Molina, M.A. Baños, J. Giméneza, S. Esplugas, Applied Catalysis: B Environmental 47 (2004) 219-256.

[25] M. Munoz, Z.M. de Pedro, J.A. Casas, J.J. Rodriguez, Journal of Hazardous Materials 190 (2011) 993-1000.

[26] M. Munoz, Z.M. de Pedro, G. Pliego, J.A. Casas, J.J. Rodriguez, Industrial & Engineering Chemistry Research 51 (2012) 13092-13099.

[27] J.A. Zazo, G. Pliego, S. Blasco, J.A. Casas, J.J. Rodriguez, Industrial & Engineering Chemistry Research 50 (2011) 866-870.

[28] G. Ovejero, J.L. Sotelo, F. Martínez, J.A. Melero, L. Gordo, Industrial & Engineering Chemistry Research 40 (2001) 3921-3928.

[29] J.A. Zazo, J.A. Casas, A.F. Mohedano, J.J. Rodriguez, Applied Catalysis B: Environmental 65 (2006) 261-268.

[30] A. Rey, M. Faraldos, J.A. Casas, J.A. Zazo, A. Bahamonde, J.J. Rodriguez, Applied Catalysis B: Environmental 86 (2009) 69-77.

[31] C. Catrinescu, D. Arsene, P. Apopei, C. Teodosiu, Applied Clay Science 58 (2012) 96-101.

[32] G. Satishkumar, M. Landau, T. Buzaglo, L. Frimet, M. Ferentz, R. Vidruk, F. Wagner, Y. Gal, M. Herskowitz, Applied Catalysis B: Environmental 138-139 (2013) 276-284.

[33] P. Bautista, A.F. Mohedano, N. Menéndez, J.A. Casas, J.A. Zazo, J.J. Rodriguez, Journal of Chemical Technology and Biotechnology 86 (2011) 497-504.

[34] M. Munoz, Z.M. de Pedro, N. Menendez, J.A. Casas, J.J. Rodriguez, Applied Catalysis B: Environmental 136-137 (2013) 218-224.

[35] L.Y. Taketa, F. Ignachewski, J.C. Villalba, F.J. Anaissi, S.T. Fujiwara, Environmental Science & Pollution Research (2014), doi: 10.1007/s11356-014-3239-3.

[36] W.P. Kwan, B.M. Voelker, Environmental Science & Technology 37 (2003) 1150-1158.

[37] R.C.C. Costa, M.F.F. Lelis, L.C.A. Oliveira, J.D. Fabris, J.D. Ardisson, R.R.V.A. Rios, C.N. Silva, R.M. Lago, Journal of Hazardous Materials 129 (2006) 171-178.

[38] P. Baldrian, V. Merhautová, J. Gabriel, F. Nerud, P. Stopka, M. Hrubý, M.J. Beneš, Applied Catalysis B: Environmental 66 (2006) 258-264.

[39] F. Magalhães, M.C. Pereira, S.E.C. Botrel, J.D. Fabris, W.A. Macedo, R. Mendonça, R.M. Lago, L.C.A. Oliveira, Applied Catalysis A: General. 332 (2007) 115-123.

[40] R. Matta, K. Hanna, S. Chiron, Science of the Total Environment 385 (2007) 242-251.

[41] J. Zhang, J. Zhuang, L. Gao, Y. Zhang, N. Gu, J. Feng, D. Yang, J. Zhu, X. Yan, Chemosphere 73 (2008) 1524-1528.

[42] H. Huang, M. Lu, J. Chen, Water Research 35 (2001) 2291-2299.

[43] G.B. Ortiz de la Plata, O.M. Alfano, A.E. Cassano, Applied Catalysis B: Environmental 95 (2010) 1-13.

[44] M. Lu, J. Chen, H. Huang, Chemosphere 46 (2002) 131-136.

[45] M.C. Pereira, L.C.A. Oliveira, E. Murad, Clay minerals 47 (2012) 285-302.

[46] K. Hanna, T. Kone, G. Medjahdi, Catalysis Communications 9 (2008) 955-959.

[47] S.R. Pouran, A.A.A. Raman, W.M.A. Daud, Journal of Cleaner Production 64 (2014) 24-35.

[48] X. Xue, K. Hanna, C. Despas, F. Wu, N. Deng, Journal of Molecular Catalysis A: Chemical 311 (2009) 29-35.

[49] K. Hanna, T. Kone, C. Ruby, Environmental Science & Pollution Research 17 (2010) 124-134.

[50] Y. Zhong, X. Liang, Y. Zhong, J. Zhu, S. Zhu, P. Yuan, H. He, J. Zhang, Water Research 46 (2012) 4633-4644.

[51] X. Liang, Y. Zhong, S. Zhu, J. Zhu, P. Yuan, H. He, J. Zhang, Journal of Hazardous Materials 181 (2010) 112-120.

[52] M. Usman, P. Faure, K. Hanna, M. Abdelmoula, C. Ruby, Fuel 96 (2012) 270-276.

[53] Du W., Xu Y., Wang Y., Langmuir 24 (2008) 175-181.

[54] T. Zhou, Y. Li, J. Ji, F. Wong, X. Lu, Separation and Purification Technology 62 (2008) 551-558.

[55] R. Matta, K. Hanna, T. Kone, S. Chiron, Chem. Eng. J. 144 (2008) 453-458.

[56] S. Aravena, C. Pizarro, M.A. Rubio, L.C.D. Cavalcante, V.K. Garg, M.C. Pereira ,J.D. Fabris, Hyperfine Interactions 195 (2010) 35–41.

[57] X. Liang, Z. He, G. Wei, P. Liu, Y. Zhong, W. Tan, P. Du, J. Zhu, H. He, J. Zhang, Journal of Colloid and Interface Science 426 (2014) 181-189.

[58] Y. Zhong, X. Liang, Z. He, W. Tan, J. Zhu, P. Yuan, R. Zhu, H. He, Applied Catalysis B: Environmental 150-151 (2014) 612-618.

[59] M. Munoz, Z.M. de Pedro, J.A. Casas, J.J. Rodriguez, Unpublished (2015).

[60] E. Moctezuma, B. Zermeño, E. Zarazua, L.M. Torres-Martínez, R. García, Topics in Catalysis 54 (2011) 496-503.

[61] T. Tao, Y. Chen, D. Zhou, H. Zhang, S. Liu, R. Amal, N. Sharma, A.M. Glushenkov, Chemistry A European Journal 19 (2013) 1091-1096.

[62] C. di Luca, F. Ivorra, P. Massa, R. Fenoglio, Industrial & Engineering Chemistry Research 51 (2012) 8979-8984.

[63] T.D. Nguyen, N.H. Phan, M.H. Do, K.T. Ngo, Journal of Hazardous Materials 185 (2011) 653-661.

[64] J.C. Tristão, F. Gomes de Mendonça, R.M. Lago, J.D. Ardisson, Environmental Science and Pollution Research (2014), doi: 10.1007/s11356-014-2554-z.

[65] J. Chun, H. Lee, S. Lee, S. Hong, J. Lee, C. Lee, J. Lee, Chemosphere 89 (2012) 1230-1237.

[66] L. Gu, N. Zhu, P. Zhou, Bioresource Technology 118 (2012) 638-642

[67] L. Gu, N. Zhu, H. Guo, S. Huang, Z. Lou, H. Yuan, J. Hazard. Mater. 246–247 (2013) 145-153, doi: http://dx.doi.org/10.1016/j.jhazmat.2012.12.012.

[68] C. Yang, D. Wang, Q. Tang, Journal of the Taiwan Institute of Chemical Engineers 45 (2014) 2584-2589.

[69] J. Barrault, M. Abdellaoui, C. Bouchoule, A. Majesté, J.M. Tatibouët, A. Louloudi, N. Papayannakos, N.H. Gangas, Applied Catalysis B: Environmental 27 (2000) L225-L230.

[70] C.B. Molina, J.A. Casas, J.A. Zazo, J.J. Rodriguez, Chemical Engineering Journal 118 (2006) 29-35.

[71] C.B. Molina, A.H. Pizarro, V.M. Monsalvo, A.M. Polo, A.F. Mohedano, J.J. Rodriguez, Separation Science and Technology 45 (2010) 1595-1602.

[72] C.B. Molina, J.A. Zazo, J.A. Casas, J.J. Rodriguez, Water Science and Technology 61 (2010) 2161-2168.

[73] M.N. Timofeeva, S.T. Khankhasaeva, S.V. Badmaeva, A.L. Chuvilin, E.B. Burgina, A.B. Ayupov, V.N. Panchenko, A.V. Kulikova, Applied Catalysis B: Environmental. 59 (2005) 243-248.

[74] A.A. Tireli, I.R. Guimarães, J.C.S. Terra, R.R. da Silva, M.C. Guerreiro, Environmental Science & Pollution Research, doi: 10.1007/s11356-014-2973-x.

[75] G. Wang, D. Wan, W. Li, Y. Lu, K. Chen, Chinese Journal of Environmental Engineering 8 (2014) 1857-1862.

[76] M. Munoz, Z.M. de Pedro, J.A. Casas, J.J. Rodriguez, Chemical Engineering Journal 228 (2013) 646-654.

[77] N.A. Zubir, C. Yacou, J. Motuzas, X. Zhang, J.C. Diniz da Costa, Nature (2014), doi: 10.1038/srep04594.

[78] Hu, J., Lo, I.M.C., Chen, G., Water Science and Technology 50 (2004) 139-146.

[79] J. Hu, G. Chen, I.M.C. Lo, Water Research 39 (2005) 4528-4536.

[80] Li, L., Fan, M., Brown, R.C., Van Leeuwen, J., Wang, J., Wang, W., Song, Y., Zhang, P., Critical Reviews in Environmental Science and Technology 36 (2006) 405-431.

[81] Y.F. Shen, J. Tang, Z.H. Nie, Y.D. Wang, Y. Ren, L. Zuo, Bioresoure Technology 100 (2009) 4139-4146.

[82] S.C.N. Tang, I.M.C. Lo, Water Research 47 (2013) 2613-2632.

[83] A. Dhakshinamoorthy, S. Navalon, M. Alvaro, H. Garcia, ChemSusChem 5 (2012) 46-64.

[84] L. Gao, J. Zhuang, L. Nie, J. Zhang, Y. Zhang, N. Gu, T. Wang, J. Feng, D. Yang, S. Perret, X. Yan, Nature Nanotechnology 2 (2007) 577-583.

[85] A. Lu, E. Salabas, F. Schüth, Angewandte Chemie International Edition 46 (2007) 1222-1244.

[86] D.E. Zhang, X.J. Zhang, Z.M. Ni, J. Song, H. Zheng, Crystal Growth and Design 7 (2007) 2117-2119.

[87] L. Hou, Q. Zhang, F. Jérôme, D. Duprez, H. Zhang, S. Royer, Applied Catalysis B: Environmental 144 (2014) 739-749.

[88] N. Wang, L. Zhu, D. Wang, M. Wang, Z. Lin, H. Tang, Ultrasonics Sonochemistry 17 (2010) 526-533.

[89] W. Wu, Q. He, C. Jiang, Nanoscale Research Letters 3 (2008) 397-415.

[90] Xu, J. Wang, Applied Catalysis B: Environmental 123-124 (2012) 117-126.

[91] S. Zhang, X. Zhao, H. Niu, Y. Shi, Y. Cai, G. Jiang, Journal of Hazardous Materials 167 (2009) 560-566.

[92] R. Huang, Z. Fang, X. Yan, W. Cheng, Chemical Engineering Journal 197 (2012) 242-249.

[93] S. Sun, X. Zeng, A.T. Lemley, Journal of Molecular Catalysis A: Chemical 371 (2013) 94-103.

[94] F. Velichkova, C. Julcour-Lebigue, B. Koumanova, H. Delmas, Journal of Environmental Chemical Engineering 1 (2013) 1214-1222.

[95] K. Rusevova, F. Kopinke, A. Georgi, Journal of Hazardous Materials 241–242 (2012) 433-440.

[96] N. Ferroudj, J. Nzimoto, A. Davidson, D. Talbot, E. Briot, V. Dupuis, A. Bée, M.S. Medjram, S. Abramson, Applied Catalysis B: Environmental. 136-137 (2013) 9-18.

[97] R. Munter, M. Trapido, Y. Veressinina, A. Goi, Ozone: Science and Engineering 28 (2006) 287-293.

[98] M.P. Holsapple, W.H. Farland, T.D. Landry, N.A. Monteiro-Riviere, J.M. Carter, N.J. Walker, K.V. Thomas,Toxicological Sciences 88 (2005) 12-17.

[99] P. Borm, F.C. Klaessig, T.D. Landry, B. Moudgil, J. Pauluhn, K. Thomas, R. Trottier, S. Wood, , Toxicological Sciences 90 (2006) 23-32.

[100] S.N. Luoma, F.R. Khan, M. Croteau, Frontiers of Nanoscience. 7 (2014) 157-193.

[101] C. Cao, L. Xiao, C. Chen, X. Shi, Q. Cao, L. Gao, Powder Technology 260 (2014) 90-97.

[102] N.N. Nassar, L.A. Arar, N.N. Marei, M.M.A. Ghanim, M.S. Dwekat, S.H. Sawalha, Environmental Nanotechnology, Monitoring & Management (2014), doi: dx.doi.org/10.1016/j.enmm.2014.09.001.

[103] N. Wang, L. Zhou, J. Guo, Q. Ye, J. Lin, J. Yuan, Applied Surface Science 305 (2014) 267-273.

[104] R.C.C. Costa, F.C.C. Moura, J.D. Ardisson, J.D. Fabris, R.M. Lago, Applied Catalysis B: Environmental 83 (2008) 131-139.

[105] Y. Wang, H. Zhao, M. Li, J. Fan, G. Zhao, Applied Catalysis B: Environmental 147 (2014) 534-545.

[106] Q. Lv, G. Li, H. Sun, L. Kong, H. Lu, X. Gao, Microporous and Mesoporous Materials 186 (2014) 7-13.

[107] M. Xia, C. Chen, M. Long, C. Chen, W. Cai, B. Zhou, Microporous and Mesoporous Materials 145 (2011) 217-223.

[108] L. Xu, J. Wang, Environmental Science & Technology 46 (2012) 10145−10153.

[109] Y. Ling, M. Long, P. Hu, Y. Chen, J. Huang, Journal of Hazardous Materials 264 (2014) 195-202.

[110] H. Niu, D. Zhang, S. Zhang, X. Zhang, Z. Meng, Y. Cai, Journal of Hazardous Materials 190 (2011) 559-565.

[111] A.E. Nogueira, I.A. Castro, A.S. Giroto, Z.M. Magriotis, Journal of Catalysts (2014), doi: dx.doi.org/10.1155/2014/712067.

[112] V. Cleveland, J. Bingham, E. Kan, Separation and Purification Technology 133 (2014) 388-395.

[113] X. Pan, Z. Fan, W. Chen, Y. Ding, H. Luo, X. Bao, Nature Materials 6 (2007) 507 - 511.

[114] J.M. Thomas, R. Raja, Accounts of Chemical Research 41 (2008) 708-720.

[115] Y. Lan, L. Yang, M. Zhang, W. Zhang, S. Wang, Applied Materials & Interfaces 2 (2010) 127-133.

[116] Z. Chen, Z. Guan, M. Li, Q. Yang, C. Li, Angewandte Chemie International Edition 50 (2011) 4913-4917.

[117] Z.M. Cui, Z. Chen, C.Y. Cao, L. Jiang, W.G. Song, Chemical Communications 49 (2013) 2332-2334.

[118] T. Zeng, X. Zhang, S. Wang, Y. Ma, H. Niu, Y. Cai, Chemistry A European Journal 20 (2014) 6474- 6481

[119] A.M. Cubillas, S. Unterkofler, T.G. Euser, B.J. M. Etzold, A.C. Jones, P.J. Sadler, P. Wasserscheid, P.S.J. Russell, Chemical Society Reviews 42 (2013) 8629-8648.

[120] M.S. Yalfani, S. Contreras, F. Medina, J. Sueiras, Applied Catalysis B: Environmental 89 (2009) 519-526.

[121] M.S. Yalfani, A. Georgi, S. Contreras, F. Medina, F. Kopinke, Applied Catalysis B: Environmental 104 (2011) 161-168.

[122] S. Contreras, M.S. Yalfani, F. Medina, J.E. Sueiras, Water Science and Technology 63 (2011) 2017-2024.

[123] J.H. Lunsford, Journal of Catalysis 216 (2003) 455-460.

[124] Q. Liu, J.C. Bauer, R.E. Schaak, J.H. Lunsford, Applied Catalysis A: General 339 (2008) 130-136.

[125] V.R. Choudhary, C. Samanta, T.V. Choudhary, Applied Catalysis A: General 308 (2006) 128-133.

[126] M. Munoz, Z.M. de Pedro, J.A. Casas, J.J. Rodriguez, Water Research 47 (2013) 3070-3080.

[127] E. Brillas, E. Mur, R. Sauleda, L. Sànchez, J. Peral, X. Domènech, J. Casado, Applied Catalysis B: Environmental 16 (1998) 31-42.

[128] C. Flox, S. Ammar, C. Arias, E. Brillas, A.V. Vargas-Zavala, R. Abdelhedi, Applied Catalysis B: Environmental 67 (2006) 93-104.

[129] I. Sirés, N. Oturan, M.A. Oturan, R.M. Rodríguez, J.A. Garrido, E. Brillas, Electrochimica Acta 52 (2007) 5493-5503.

[130] E. Brillas, I. Sirés, M.A. Oturan, Chemical Reviews 109 (2009) 6570-6631.

[131] M. Luo, S. Yuan, M. Tong, P. Liao, W. Xie, X. Xu, Water Research 48 (2014) 190-199.

[132] C.K. Duesterberg, W.J. Cooper, T.D. Waite, Environmental Science & Technology 39 (2005) 5052-5058.

[133] C.K. Duesterberg, T.D. Waite, Environmental Science & Technology 41 (2007) 4103-4110.

[134] J. Beltran De Heredia, J. Torregrosa, J.R. Dominguez, J.A. Peres, Chemosphere 45 (2001) 85-90.

[135] W. Wang, Y. Liu, T. Li, M. Zhou, Chemical Engineering Journal 242 (2014) 1-9.

[136] L. Zhou, Y. Shao, J. Liu, Z. Ye, H. Zhang, J. Ma, Y. Jia, W. Gao, Y. Li, Applied Materials & Interfaces 6 (2014) 7275-7285.

Table 1

Table 1. Main reactions involved in Fenton chemistry.

	Eq.	Reaction	rate constant (M^{-1} s^{-1})	Ref.
Initiation	1	$Fe^{2+} + H_2O_2 \rightarrow Fe^{3+} + HO\cdot + OH^-$	55	(Duersterberg, 2005, 2007)[132, 133]
	2	$Fe^{3+} + H_2O_2 \rightarrow Fe^{2+} + HOO\cdot + H^+$	$2.00 \cdot 10^{-3}$	(Duersterberg, 2005, 2007)[132, 133]
Propagation	3	$H_2O_2 + HO\cdot \rightarrow HOO\cdot + H_2O$	$3.30 \cdot 10^{7}$	(Duersterberg, 2005, 2007)[132, 133]
	4	$RH + HO\cdot \rightarrow R\cdot + H_2O$		Beltrán de Heredia 2001[134]
	5	$R\cdot + Fe^{2+} \rightarrow RH + Fe^{3+}$		Beltrán de Heredia 2001[134]
	6	$R\cdot + Fe^{3+} \rightarrow R^+ + Fe^{2+}$		Beltrán de Heredia 2001[134]
Termination	7	$R\cdot + R\cdot \rightarrow R–R$		Beltrán de Heredia 2001[134]
	8	$Fe^{3+} + HOO\cdot \rightarrow Fe^{2+} + O_2 + H^+$	$7.82 \cdot 10^{5}$	(Duersterberg, 2005, 2007)[132, 133]
	9	$Fe^{2+} + HO\cdot \rightarrow Fe^{3+} + OH^-$	$3.20 \cdot 10^{8}$	(Duersterberg, 2005, 2007)[132, 133]
	10	$Fe^{2+} + HOO\cdot \rightarrow Fe^{3+} + H_2O_2$	$1.34 \cdot 10^{6}$	(Duersterberg, 2005, 2007)[132, 133]
	11	$HOO\cdot + HOO\cdot \rightarrow H_2O_2 + O_2$	$2.33 \cdot 10^{6}$	(Duersterberg, 2005, 2007)[132, 133]
	12	$HO\cdot + HO\cdot \rightarrow H_2O + O_2$	$7.15 \cdot 10^{9}$	(Duersterberg, 2005, 2007)[132, 133]
	13	$HO\cdot + HO\cdot \rightarrow H_2O_2$	$5.20 \cdot 10^{9}$	(Duersterberg, 2005, 2007)[132, 133]

Table 2

Table 2. Overview of the application of magnetic iron minerals in CWPO for the removal of non-biodegradable organic pollutants.

Mineral	Composition	Target pollutant	Operating conditions	Results	Stability	Reference
Ferrihyidrite, hematite, goethite, lepidocrocite, magnetite, pyrite	Pure ferrihydrite ($Fe_2(OH)_6$) Pure hematite (Fe_2O_3) Pure goethite (α-FeOOH) Pure lepidocrocite (γ-FeOOH) Pure magnetite (Fe_3O_4) Pure pyrite (FeS_2)	2,4,6-trinitrotoluene	$C_{cont\text{-}cat\text{-}H2O2}$ = 0.025 – 1.76 – 2.7 g L^{-1} T = 25 ºC P = 1 atm pH = 3	$X_{cont\text{-}ferrihydrite}$ <10% $X_{cont\text{-}hematite}$ <10% $X_{cont\text{-}goethite}$ <10% $X_{cont\text{-}lepidocrocite}$ <10% $X_{cont\text{-}magnetite}$ = 85% $X_{cont\text{-}pyrite}$ = 100% (t = 6 h)	Iron leaching : -Ferrihydrite, hematite, goethite and lepidocrocite: 1 μg L^{-1} -Magnetite: 14 mg L^{-1} -Pyrite: 77 mg L^{-1}	Matta et al. (2007) [40]
Mixed oxides of iron and silica	Quartz/amorphous iron (III) oxide (Q_1) (59.6% iron oxide) Quartz/maghemite (Q_2) (50.7% iron oxide) Quartz/magnetite (Q_3) (59.5% iron oxide) Quartz/goethite (Q_4) (53% iron oxide)	Mehtyl red	C_{cont} = 0.025 H_2O_2/Fe molar ratio = 20 T = 20 ºC P = 1 atm pH = 5	$X_{cont\text{-}Q1}$ = 90% $X_{cont\text{-}Q2}$ = 25% $X_{cont\text{-}Q3}$ = 20% $X_{cont\text{-}Q4}$ = 100% (t = 3 h)	No significant change in Fe content or XRD patterns after use.	Hanna et al. (2008) [46]
Magnetite	Pure magnetite (Fe_3O_4)	Pentachloro- phenol	$C_{cont\text{-}cat\text{-}H2O2}$ = 0.05 – 2 – 5 g L^{-1} T = 20 ºC P = 1 atm pH = 7	X_{cont} = 90% (t = 9 h) The kinetic rate constant increased with the addition of chelating agents: EDTA>>Oxalate>CMCD >without catalyst	Iron leaching < 14 mg L^{-1}	Xue et al. (2009) [48]
Natural vanadium-titanium magnetite	Titanomagnetite (Fe_2TiO_4) (%) = 76 Magnetite (Fe_3O_4) (%) = 12 Chlorite ($(Mg,Fe,Li)_6AlSi_3O_1$	Acid Orange II	$C_{cont\text{-}cat\text{-}H2O2}$ = 0.07 – 1 – 0.34 g L^{-1} T = 25 ºC P = 1 atm	X_{cont} = 98% (t = 4 h)	3 runs $X_{cont(1st)}$ = 98% $X_{cont(2nd)}$ = 93% $X_{cont(3rd)}$ = 90%	Liang et al. (2010) [51]

	$_0(OH)_8$) (%) = 12		pH = 3			
Titanomagnetite (UV/Fenton)	$Fe_{2.02}Ti_{0.98}O_4$	Tetrabromobis-phenol A	$C_{cont\text{-}cat\text{-}H2O2}$ = 0.02 – 0.125 – 0.34 g L^{-1} T = 25 ºC P = 1 atm pH = 6.5 (UV 6W λ=365 nm)	X_{cont} = 100% (t = 4 h)	3 runs $X_{cont(1st)}$ = 100% $X_{cont(3rd)}$ = 90%	Zhong et al. (2012) [50]
Magnetite rich sandy soil (MRS)	Magnetite (Fe_3O_4) (%) = 10	Oil hydrocarbon	$C_{cont\text{-}cat\text{-}H2O2}$ = 0.4 – 100 – 10 g L^{-1} T = 25 ºC P = 1 atm pH = 6.7	X_{cont} > 80% (one week)	Not studied	Usman et al. (2012) [52]
Magnetite, hematite, ilmenite	Pure magnetite (Fe_3O_4) Pure hematite (Fe_2O_3) Pure ilmenite ($FeTiO_3$)	Phenol	$C_{cont\text{-}cat\text{-}H2O2}$ = 0.1 – 1 – 0.5 g L^{-1} T = 25-90 ºC P = 1 atm pH = 3	X_{cont} = 100% (t = 2 h) X_{TOC} > 70% (t = 4 h) (T = 75 ºC; similar results with the three minerals)	3 runs (Fe_3O_4- Fe_2O_3-$FeTiO_3$) $X_{TOC(1st)}$ = 71%-78%-71% $X_{TOC(2nd)}$ = 72%-72%-1% $X_{TOC(3rd)}$ = 77%-69%-1%	Munoz et al. (2015), unpublished [59]

Table 3

Table 3. Summary of the works reported in the literature relative to the synthesis of magnetic catalysts by *in-situ* growth of magnetite and their application in CWPO.

Catalyst	Target pollutant	Operating conditions	Results	Stability	Reference
Magnetic Fe_2MO_4 activated carbon	Methyl orange	$C_{cont\text{-}cat\text{-}H2O2}$ = 0.05 – 2.5 – 0.6 g L^{-1} T = 30 ºC P = 1 atm pH = 4	X_{cont} = 100% X_{TOC} = 59% (t = 2 h)	3 runs $X_{cont(1st)}$ = 100% $X_{cont(2nd)}$ = 95% $X_{cont(3rd)}$ = 85% Iron leaching: 0.47, 0.30 and 0.26 mg L^{-1} for 1, 2 and 3 runs	Nguyen et al. (2011) [63]
Magnetite/ mesocellular carbon foam	Phenol	$C_{cont\text{-}cat\text{-}H2O2}$ = 0.01 – 0.1 – 0.34 g L^{-1} T = 20 ºC P = 1 atm pH = 3	X_{cont} = 95% (t = 4 h)	Multiple runs Non appreciable loss of activity Iron leaching < 0.6 mg L^{-1}	Chun et al. (2012) [65]
Sewage sludge derived magnetic porous carbon	1-diazo-2-naphtol-4-sulfonic acid	$C_{cont\text{-}cat\text{-}H2O2}$ = 0.25 – 0.5 – 0.5 g L^{-1} T = 25 ºC P = 1 atm pH = 5	X_{cont} = 97% X_{TOC} = 87% (t = 4 h)	3 runs $X_{cont(1st)}$ = 97% $X_{cont(3rd)}$ = 90%	Gu et al. (2012) [66]
Sewage sludge derived magnetic porous carbon	1-diazo-2-naphtol-4-sulfonic acid	$C_{cont\text{-}cat\text{-}H2O2}$ = 0.15 – 0.5 – 0.51 g L^{-1} T = 25 ºC P = 1 atm pH = 5	X_{cont} = 94% X_{TOC} = 48% (t = 2 h)	Iron leaching < 7.4 ng L^{-1}	Gu et al. (2013) [67]
Ferromagnetic γ-Al_2O_3-supported iron catalyst (Fe_3O_4/γ-Al_2O_3)	4-chlorophenol (4-CP) 2,4-dichlorophenol (2,4-DCP) 2,4,6-trichlorophenol (2,4,6-TCP)	$C_{cont\text{-}cat\text{-}H2O2}$ = 0.1 – 1.0 – 0.35 (4-CP), 0.21 (2,4-DCP), 0.18 (2,4,6-TCP) g L^{-1} T = 50 ºC P = 1 atm pH = 3	X_{cont} = 100% (1, 2, 3 h for 4-CP, 2,4-DCP and 2,4,6-TCP, respectively) X_{TOC} >75% (t = 4h)	Long-term continuous experiment (100 h). No loss of activity. Iron leaching <2.5 mg L^{-1}	Munoz et al. (2013) [34]
Reactive Fe particles dispersed	Methylene blue	$C_{cont\text{-}cat\text{-}H2O2}$ = 0.2 – 4.3 – 86	X_{cont} = 95%	Not studied	Tristao et al. (2014)

in a carbon matrix		g L^{-1} T = 26 ºC P = 1 atm pH = 6	(t = 3 h)		[64]
Magnetic porous carbon microspheres	Methylene blue	$C_{cont\text{-}cat\text{-}H2O2}$ = 0.04 – 2 – 0.54 g L^{-1} T = 30 ºC P = 1 atm pH = 5	X_{cont} = 100% X_{TOC} = 65% (t = 0.67 h)	10 runs $X_{cont\ (10th)}$ = 100% $X_{TOC(10th)}$ = 55% Iron leaching 0.5 mg L^{-1}	Zhou et al. (2014) [136]
Magnetic iron oxide-pillared clay	Methylene blue	$C_{cont\text{-}cat\text{-}H2O2}$ = 0.05 – 0.375 – 1 g L^{-1} T = 25 ºC P = 1 atm pH = 6	X_{cont} = 47% (t = 2.5 h)	Not studied	Tireli et al., (2014) [74]
Magnetic bentonite	Orange II	$C_{cont\text{-}cat\text{-}H2O2}$ = 0.175 – 0.6 – 0.71 g L^{-1} T = 40 ºC P = 1 atm pH = 3	X_{cont} = 100% (t = 3 h)	4 runs $X_{cont(1st)}$ = 100% $X_{cont(5th)}$ = 100%	Wang et al. (2014a) [75]
NdFeB magnetic activated carbon	Methyl orange	$C_{cont\text{-}cat\text{-}H2O2}$ = 0.02 – 10 – 0.02 g L^{-1} T = 20 ºC P = 1 atm pH = 3	X_{cont} = 98% (t = 1 h)	5 runs $X_{cont(1st)}$ = 98% $X_{cont(5th)}$ = 97%	Yang et al., (2014) [68]

Table 4

Table 4. Summary of the studies devoted to the application of unsupported MNPs in CWPO.

Catalyst	Target pollutant	Operating conditions	Results	Stability	Reference
Ferromagnetic nanoparticles	Phenol	$C_{cont\text{-}cat\text{-}H2O2}$ = 0.28 – 0.1 – 2 g L^{-1} T = 16 ºC P = 1 atm pH = 3	X_{cont} = 85% X_{TOC} < 30% (t = 3 h)	After 5 runs, still remained almost 100% of the MNPs activity	Zhang et al. (2008) [41]
Ferromagnetic nanoparticles	Phenol Aniline	$C_{cont\text{-}cat\text{-}H2O2}$ = 0.094 – 5 – 40 g L^{-1} T = 35 ºC P = 1 atm pH = 7	X_{phenol} = 100% $X_{aniline}$ = 100% $X_{TOC(phenol)}$ = 43% $X_{TOC(aniline)}$ = 40% (t = 6 h)	After 8 runs, X_{phenol} was reduced by 20% and X_{TOC} by 30%.	Zhang et al. (2009) [91]
Ferromagnetic nanoparticles	Rhodamine B	$C_{cont\text{-}cat\text{-}H2O2}$ = 0.01 – 0.6 – 1.4 g L^{-1} T = 40 ºC P = 1 atm pH = 5.4 (Fe^{2+}/Fe^{3+} 1:1 ratio in synthesis)	X_{cont} = 90% (t = 1 h)	Iron leaching < 0.015 mg L^{-1}	Wang et al. (2010) [88]
Ferromagnetic nanoparticles (Sono-Fenton)	Bisphenol A	$C_{cont\text{-}cat\text{-}H2O2}$ = 0.02 – 0.6 – 5.4 g L^{-1} T = 35 ºC P = 1 atm pH = 5 (Ultrasound at 40 kHz, 100 w)	X_{cont} = 100% X_{TOC} = 49% (t = 8 h)	5 runs $X_{cont(5th)}$ = 70% Loss of MNPs (0.5 mg L^{-1}/run)	Huang et al. (2012) [92]
Nano-sized magnetic iron oxides	Phenol	$C_{cont\text{-}cat\text{-}H2O2}$ = 0.025 – 3 – 5 g L^{-1} T = 22 ºC P = 1 atm pH = 7	X_{cont} = 60% (t = 24 h)	3 runs $X_{cont(1st)}$ = 60% $X_{cont(2nd)}$ = 55% $X_{cont(3rd)}$ = 30% Iron leaching <0.01 mg L^{-1}/run	Rusevova et al. (2012) [95]

Ferromagnetic nanoparticles	2,4-dichlorophenol	$C_{cont-cat-H2O2}$ = 0.1 – 1 – 0.4 g L^{-1} T = 30 ºC P = 1 atm pH = 3	X_{cont} = 100% X_{TOC} = 51% (t = 3 h)	5 runs $X_{cont(1st)}$ = 95% $X_{cont(3rd)}$ = 60% $X_{cont(5th)}$ = 40% (t = 2 h) Iron leaching = 9.8 mg L^{-1}	Xu and Wang (2012) [90]
Maghemite nanoparticles (NP) and maghemite/silica nanocomposite microspheres (MS)	Methyl orange (MO) Methylene blue (MB) Paranitrophenol (PNP)	$C_{cont-cat-H2O2}$ = 0.08 (MO,MB), 0.035 (PNP) – 1.75 (Fe) – 34 g L^{-1} T = 40 ºC P = 1 atm pH = 6.5	X_{NP-MO} = 100% X_{NP-MB} = 82% X_{NP-PNP} = 72% X_{MS-MO} = 96% X_{MS-MB} = 98% X_{MS-PNP} = 67% (t = 4 h)	5 runs $X_{MS-MO(1st)}$ = 95% $X_{MS-MO(3rd)}$ = 92% $X_{MS-MO(5th)}$ = 90% Iron leaching = 7.3 mg L^{-1}	Ferroudj et al. (2013) [96]
Nanostructured magnetite (MGN1) Submicrostructured magnetite (MGN2) Nanostructured maghemite (MGM)	Paracetamol	$C_{cont-cat-H2O2}$ = 0.1 – 6 – 0.95 g L^{-1} T = 60 ºC P = 1 atm pH = 2.6	X_{cont} = 100% X_{TOC} ≈ 50% (t = 5 h)	2 cycles MGN1: $X_{TOC(2nd)}$ ≈ 50% MGN2: $X_{TOC(2nd)}$ ≈ 50% MGM: $X_{TOC(2nd)}$ = 34% Iron leaching < 1% MGN1: 7.4 mg L^{-1} MGN2: 3.8 mg L^{-1} MGM: 7.6 mg L^{-1}	Velichkova et al. (2013) [94]
Ferromagnetic nanoparticles (MNPs)	Carbmazepine (CBZ) Ibuprofen (IBP)	$C_{cont-cat-H2O2}$ = 0.015 – 1.84 – 20.4 g L^{-1} T = 23 ºC P = 1 atm pH = 7	X_{CBZ} = 86% X_{IBP} = 83% (t = 12 h)	Not studied	Sun et al. (2013) [93]

Table 5

Table 5. Summary of the application of supported MNPs and magnetic composites in Fenton oxidation.

Catalyst	Target pollutant	Operating conditions	Results	Stability	Reference
Fe^0/Fe_3O_4 composite	Methylene blue	$C_{cont-cat-H2O2}$ = 0.1 – 3 – 10 g L^{-1} T = 25 ºC P = 1 atm pH = 6	X_{TOC} = 75% (t = 2 h)	Not studied	Costa et al. (2008) [104]
Magnetic mesoporous silica nanocomposite	Phenol	$C_{cont-cat-H2O2}$ = 0.2 – 5 – 1.7 g L^{-1} T = 40 ºC P = 1 atm pH = 4	X_{TOC} = 78% (t = 2 h)	3 runs $X_{TOC(1st)}$ = 78% $X_{TOC(3rd)}$ = 65% Iron leaching: 0.9 to 0.29 mg L^{-1} from 1 to 3 run	Xia et al. (2011) [107]
Humic acid coated Fe_3O_4 magnetic nanoparticles	Sulfathiazole	$C_{cont-cat-H2O2}$ = 0.05 – 3 – 14 g L^{-1} T = 40 ºC P = 1 atm pH = 3.5	X_{cont} = 100% (t = 1 h) X_{TOC} > 90% (t = 6 h)	3 runs $X_{cont(1-3\ runs)}$ = 100% (t = 6 h) Iron leaching < 0.1 mg L^{-1}	Niu et al. (2011) [110]
Magnetic nanoscaled Fe_3O_4/CeO_2 composite	4-chlorophenol	$C_{cont-cat-H2O2}$ = 0.1 – 2 – 1 g L^{-1} T = 30 ºC P = 1 atm pH = 3	X_{cont} = 100% (t = 1 h)	6 runs $X_{cont(1st)}$ = 100% $X_{cont(3rd)}$ = 60% $X_{cont(6th)}$ = 40% (t = 1 h) High iron leaching = 12 mg L^{-1}	Xu and Wang (2012) [108]
Shape-controlled nanostructures magnetite-type materials	Phenol	$C_{cont-cat-H2O2}$ = 0.6 – 0.3 – 1.36 g L^{-1} T = 25 ºC P = 1 atm pH = 4	X_{cont} = 98% X_{TOC} = 74% (t = 1.5 h)	3 runs $X_{cont(1st)}$ = 98% $X_{cont(3rd)}$ = 93% $X_{TOC(1st)}$ = 74% $X_{TOC(3rd)}$ = 68% Iron leaching = 0.17 mg L^{-1}/run Reasons: -partial oxidation	Hou et al. (2014) [87]

				of Fe^{2+} to Fe^{3+}	
Magnetic core-shell structural γ-Fe_2O_3@Cu/Al-MCM-41 nanocomposite	Phenol	$C_{cont-cat-H2O2}$ = 0.08 – 1 – 1.7 g L^{-1} T = 40 ºC P = 1 atm pH = 4	X_{TOC} = 80% (t = 2 h)	3 runs $X_{TOC(1st)}$ = 80% $X_{TOC(2nd)}$ = 60% $X_{TOC(3rd)}$ = 40% Leaching: Cu^{2+}= 0.18 mg L^{-1} Fe^{3+} = 0.12 mg L^{-1}	Ling et al. (2014) [109]
Magnetic core/shell structured g-Fe_2O_3@Ti-tmSiO_2	Methylene blue	$C_{cont-cat-H2O2}$ = 0.05 – 0.05 – 15 g L^{-1} T = 25 ºC P = 1 atm pH = 4	X_{cont} = 99% (t = 5.5 h)	6 runs No loss of activity Iron leaching = 0.17 mg L^{-1}	Lv et al. (2014) [106]
Magnetic composite nanospheres	Phenol	$C_{cont-cat-H2O2}$ = 0.21 – 0.1 – 1.36 g L^{-1} T = 20 ºC P = 1 atm pH = 5	X_{cont} = 98% X_{COD} = 76% (t = 2 h)	3 runs $X_{cont(1st)}$ = 98% $X_{COD(1st)}$ = 76% $X_{cont(3rd)}$ = 95% $X_{COD(3rd)}$ = 70% Iron leaching = 3%	Wang et al. (2014c) [135]
Graphene oxide-Fe_3O_4 nanocomposites	Acid orange 7	$C_{cont-cat-H2O2}$ = 0.035 – 0.2 – 0.75 g L^{-1} T = 25 ºC P = 1 atm pH = 3	X_{cont} = 100% (t = 3 h)	Not studied	Zubir et al. (2014) [77]
Magnetic ordered mesoporous copper ferrite (Meso-$CuFe_2O_4$)	Imidacloprid	$C_{cont-cat-H2O2}$ = 0.01 – 0.3 – 1.36 g L^{-1} T = 30 ºC P = 1 atm pH = 3	X_{cont} = 100% X_{TOC} = 33% (t = 5 h)	5 runs $X_{cont(1st)}$ = 100% $X_{cont(5th)}$ = 100% Iron leaching <1 mg L^{-1}	Wang et al. (2014b) [105]
Magnetic nanocomposite (Magnetite/ MCM-41)	Methylene blue	$C_{cont-cat-H2O2}$ = 0.05 – 10 – 3.3 g L^{-1} T = 25 ºC P = 1 atm pH = natural	X_{cont} = 50% X_{TOC} = 43% (t = 3 h)	4 runs $X_{TOC\ (4th)}$ = 38%	Nogueira et al., (2014) [111]

Multi-walled carbon nanotube-supported Fe_3O_4 (Fe_3O_4/MWCNT)	Bisphenol A	$C_{cont\text{-}cat\text{-}H2O2}$ = 0.07 – 0.5 – 0.04 g L^{-1} T = 50 ºC P = 1 atm pH = 3	X_{cont} = 97% X_{COD} = 35% (t = 6 h)	5 runs $X_{cont(1st)}$ = 90% $X_{COD(1st)}$ = 35% $X_{cont(5th)}$ = 90% $X_{COD(5th)}$ = 25%	Cleveland et al., (2014) [112]

Figure 1

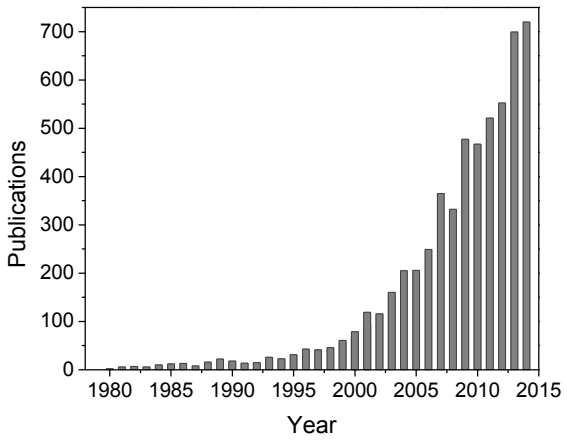

Figure 1. Evolution of the number of scientific papers devoted to the application of Fenton oxidation to wastewater treatment. Source: *Scopus (December 2014)*.

Figure 2

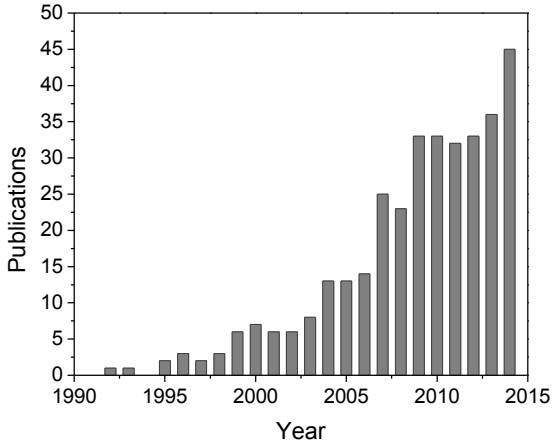

Figure 2. Evolution of the number of scientific papers devoted to the application of CWPO to wastewater treatment. Source: *Scopus (December 2014)*.

Figure 3

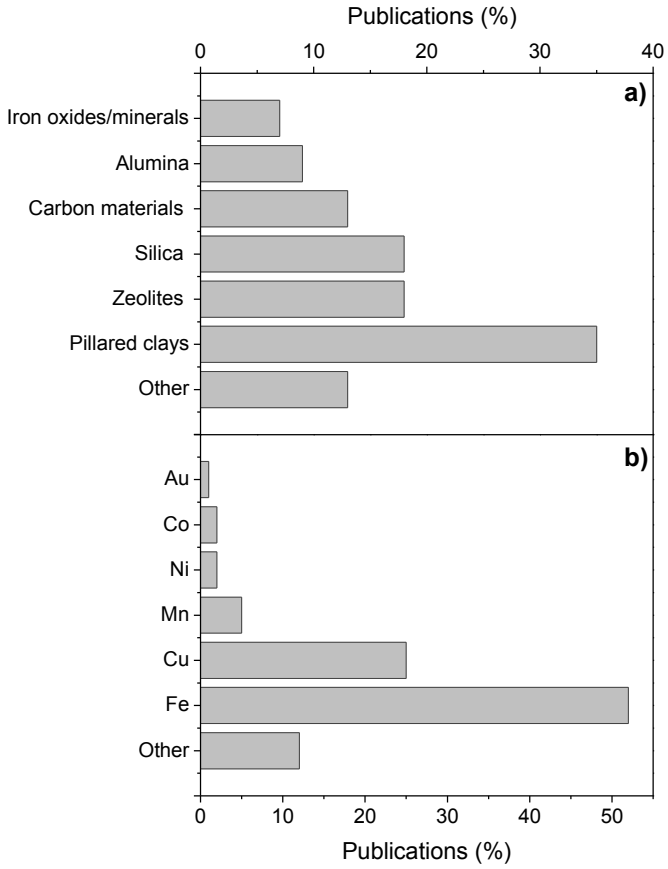

Figure 3. Literature generated in the field of CWPO by sort of catalytic supports (a) and metal active phase (b) studied. Source: *Scopus (December 2014)*.

Figure 4

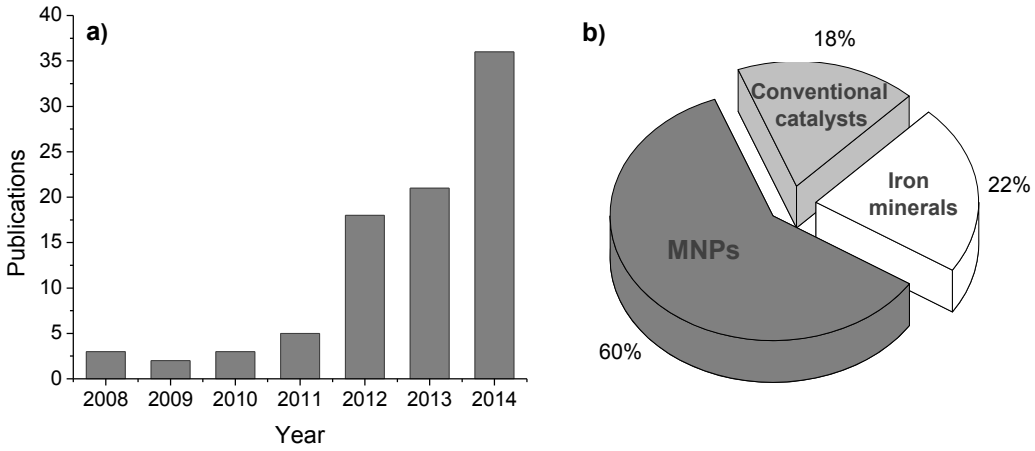

Figure 4. Evolution of the number of publications dealing with the application of magnetic materials as catalysts in Fenton oxidation (a) and their distribution according to the kind of magnetic material used (b). Source: *Scopus (December 2014)*.

Figure 5

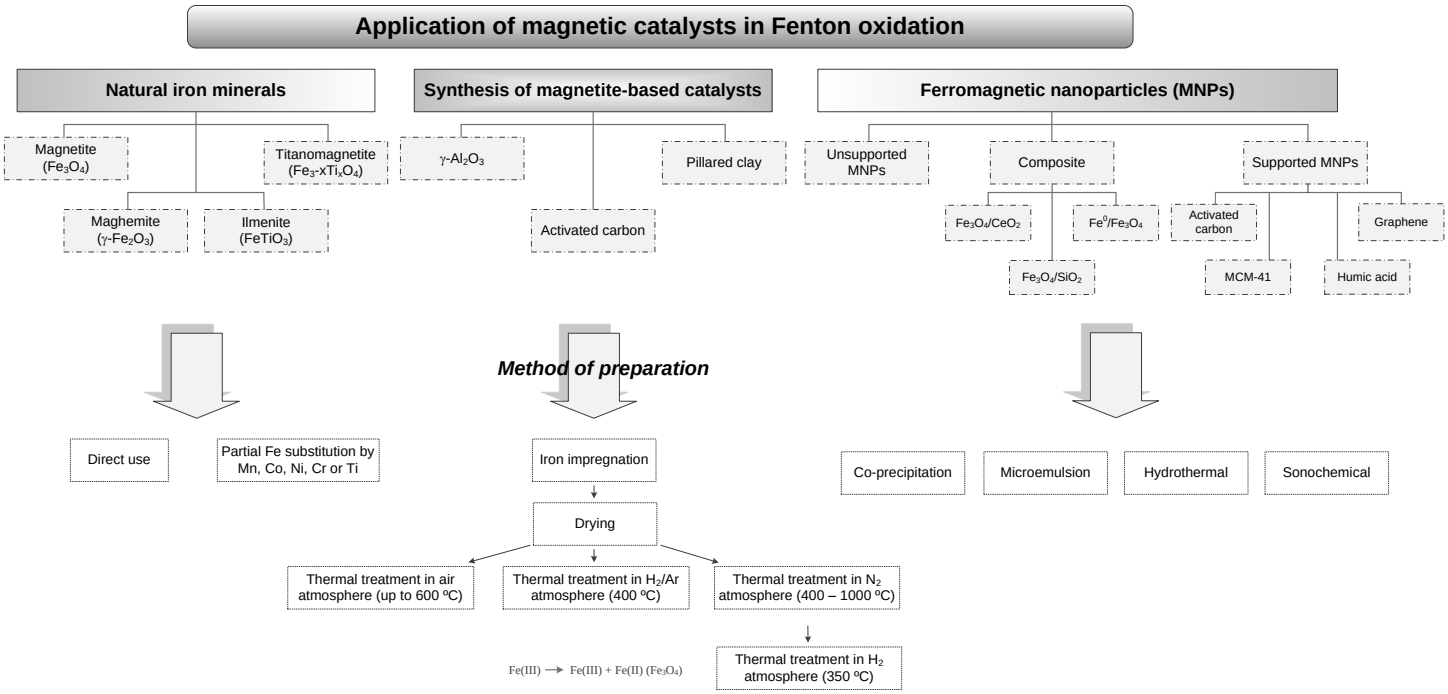

Figure 5. Trends distinguished in the investigation of magnetic catalysts for CWPO, including the materials and preparation methods involved.